# IMPAD1 and KDELR2 drive NSCLC invasion and metastasis by enhancing Golgi-mediated secretion

Rakhee Bajaj, Samrat T. Kundu, Caitlin L. Grzeskowiak, Jared J. Fradette, Kenneth L. Scott, Chad J. Creighton, Don L. Gibbons

# Supplemental Fig. 1

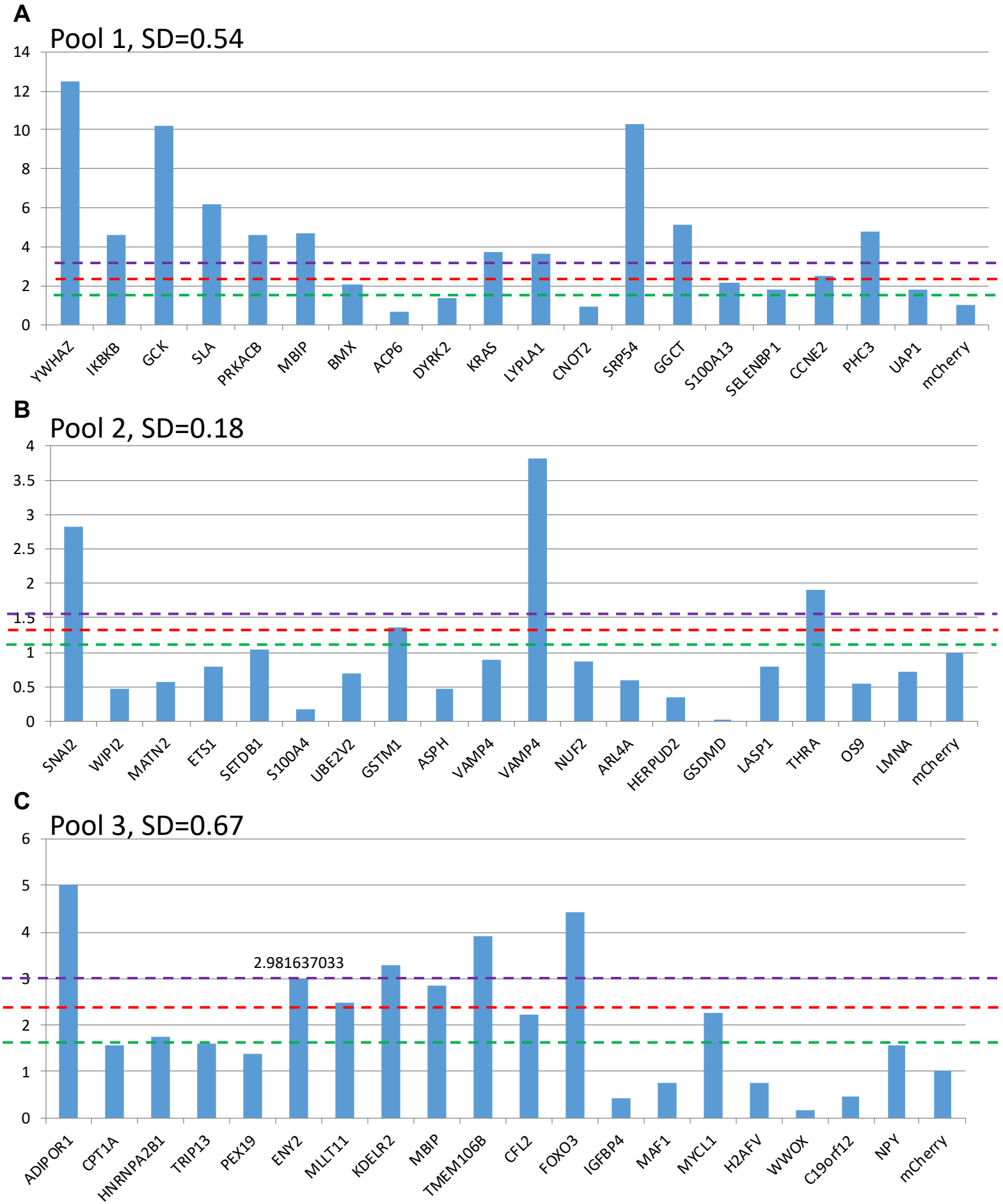

# Supplemental Fig. 1

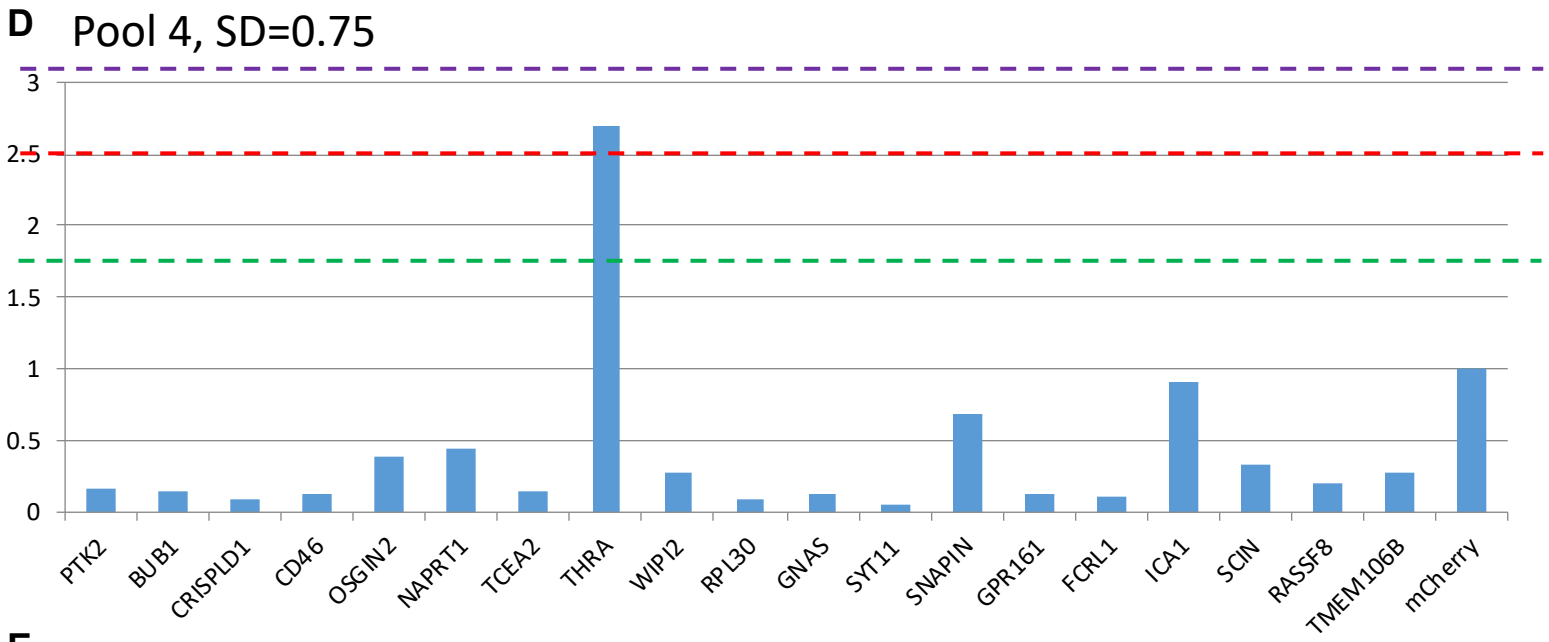


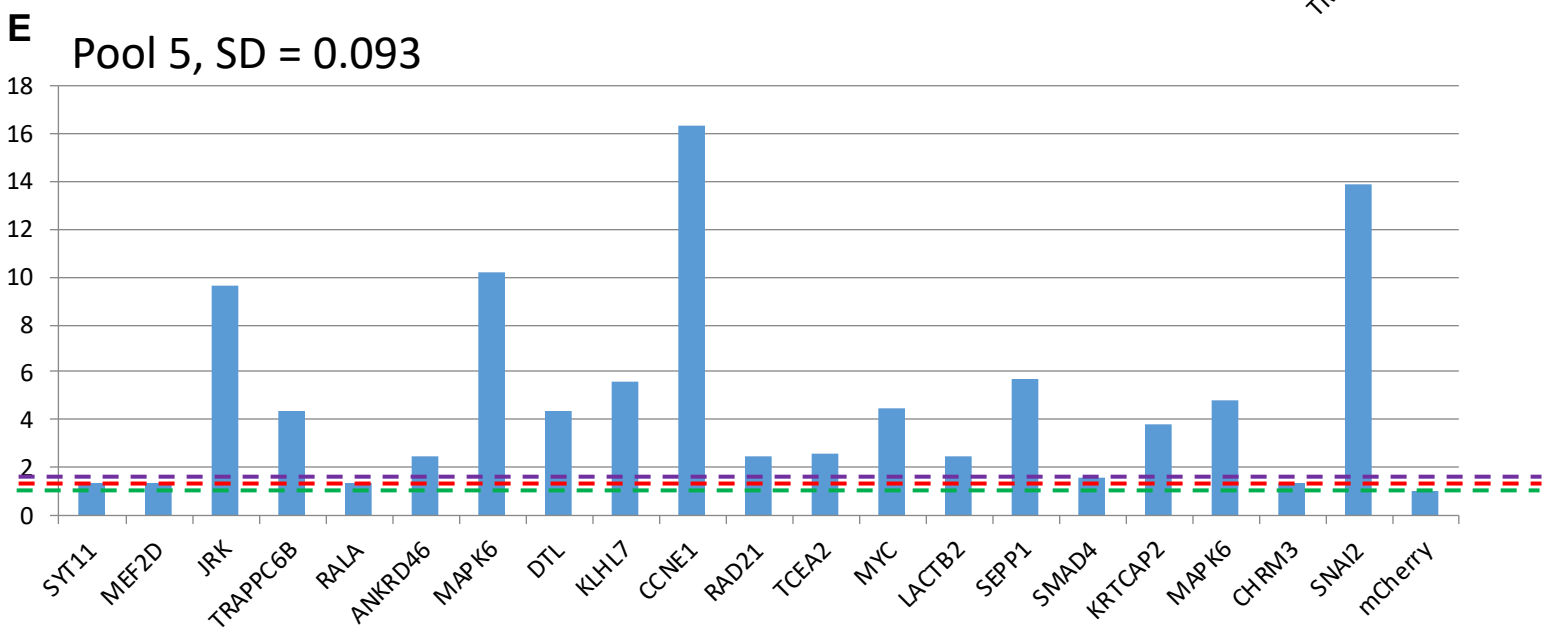


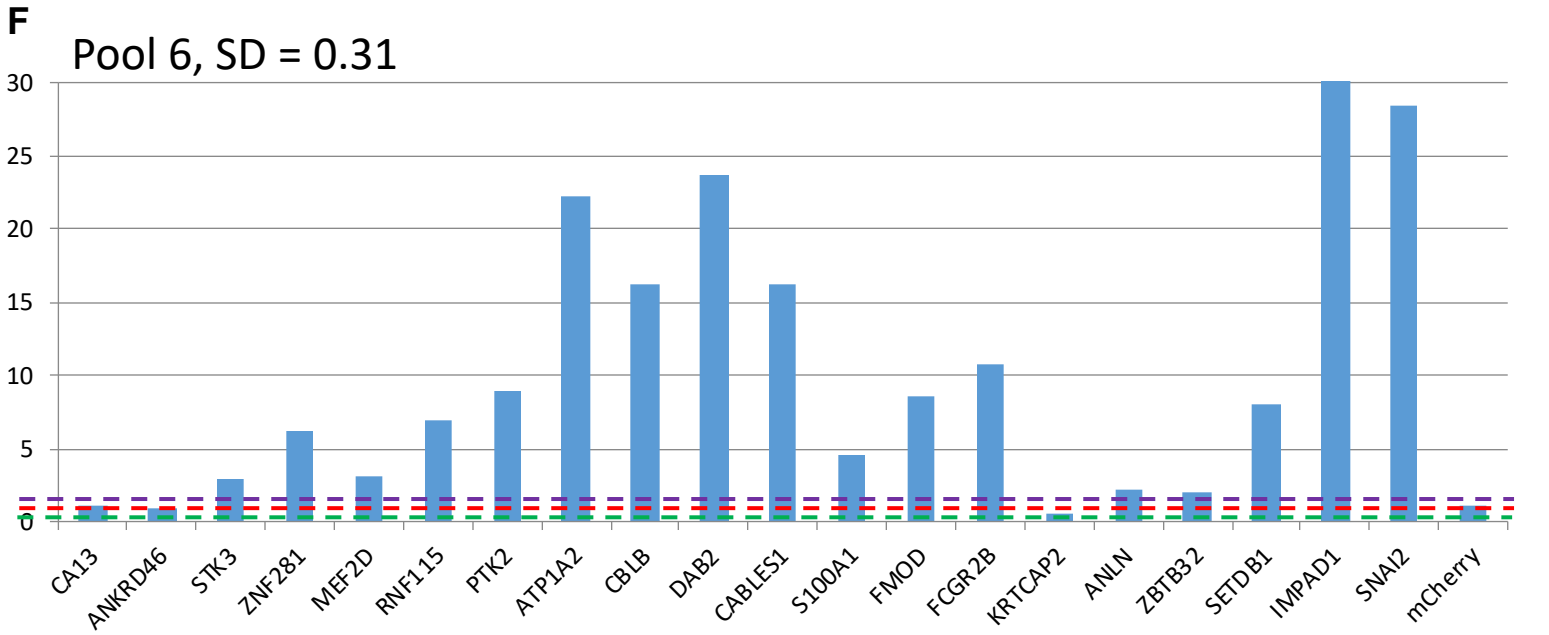

# Supplemental Fig. 1

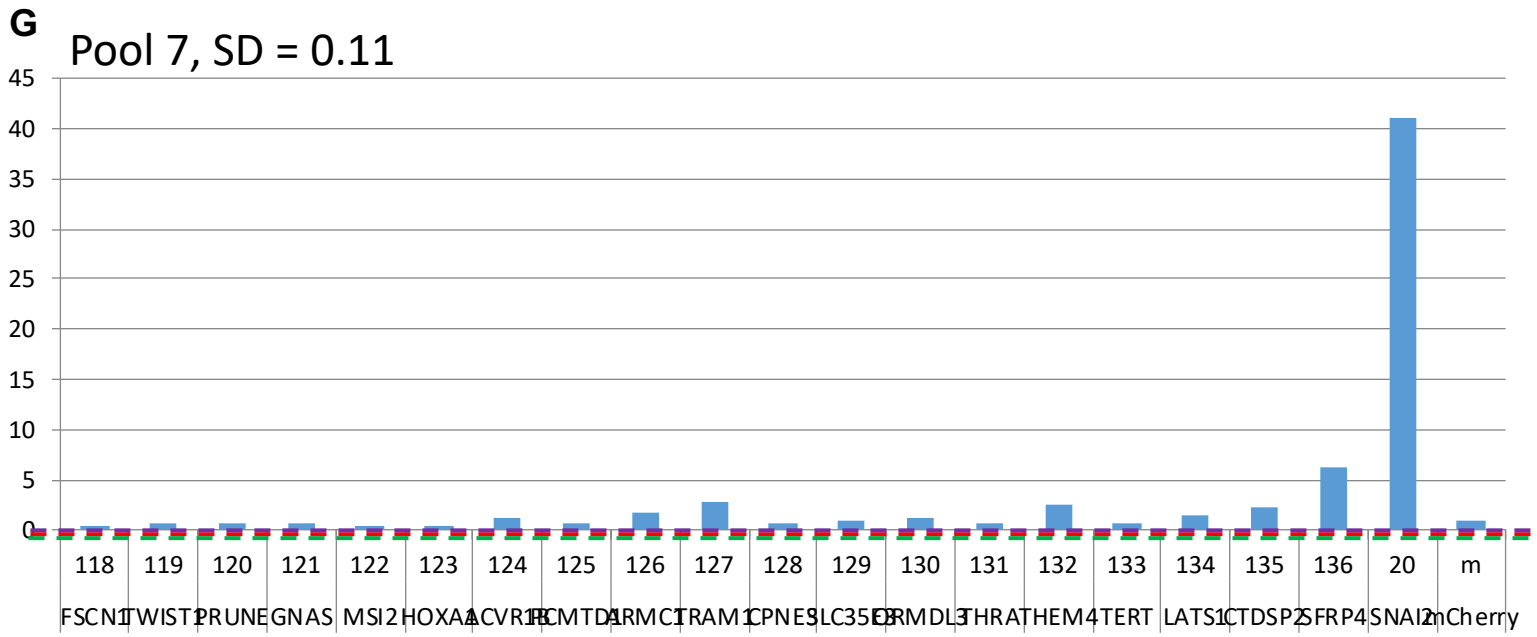


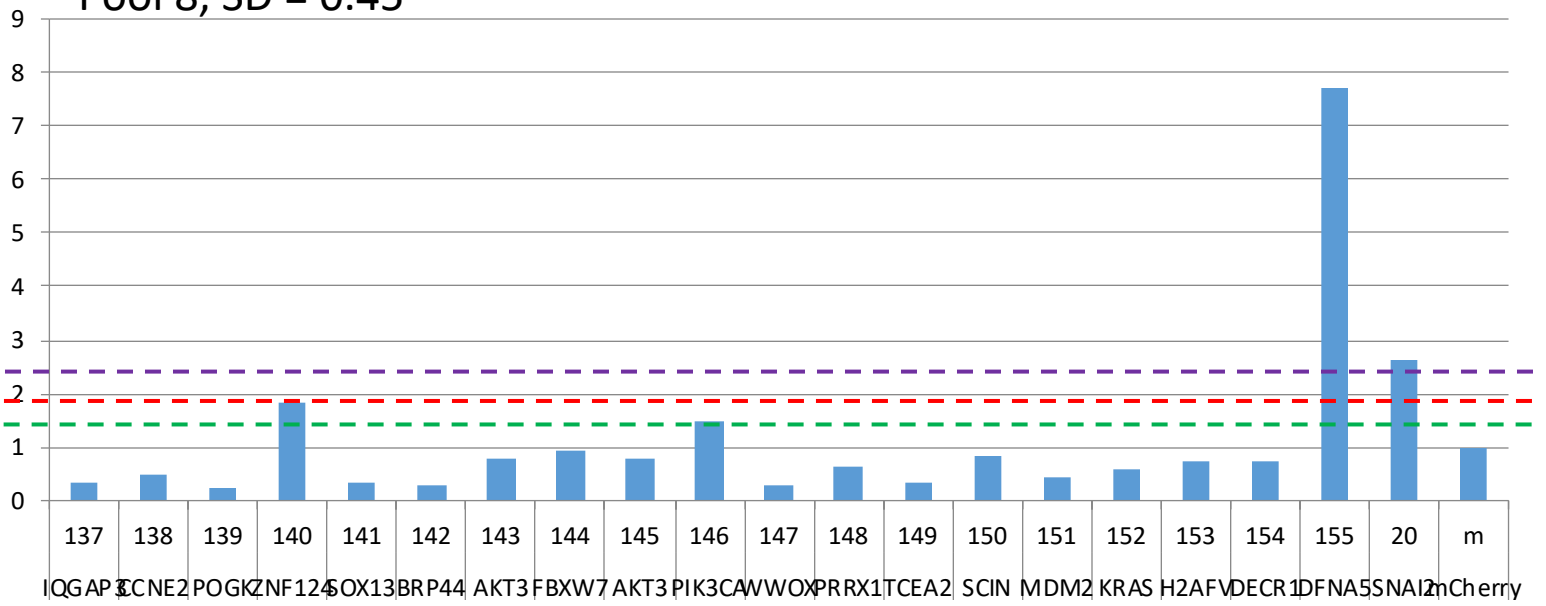


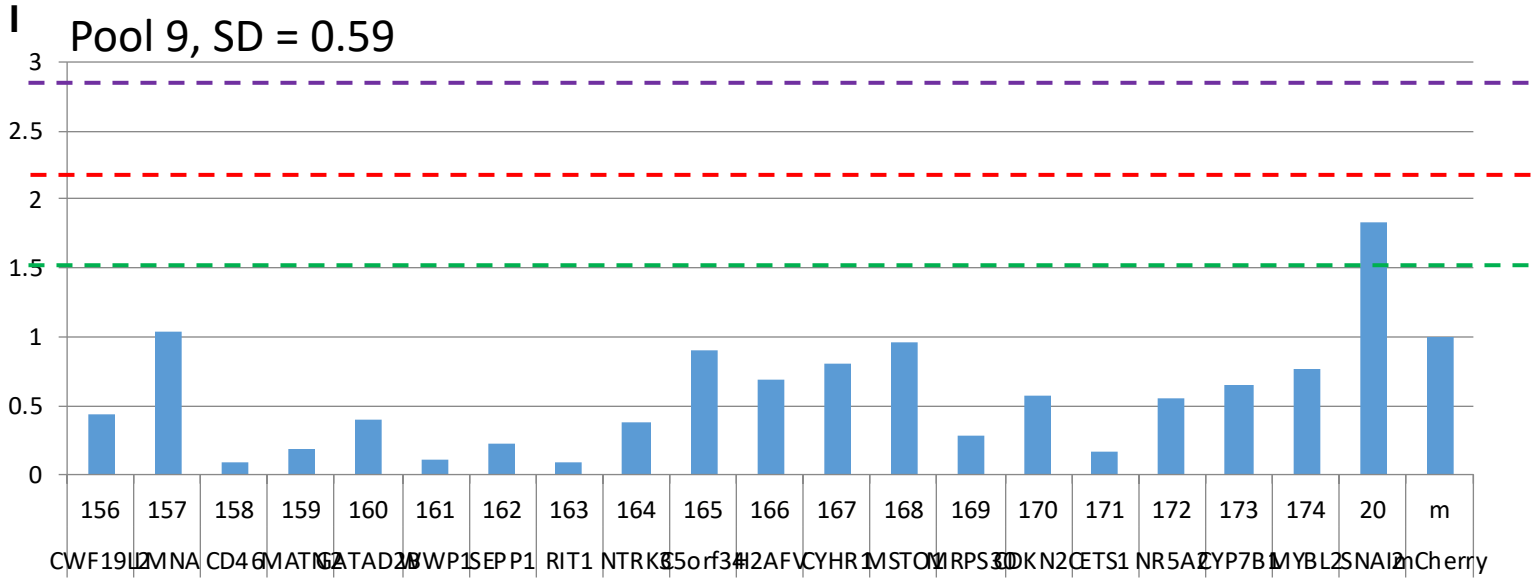

# Supplemental Fig. 1

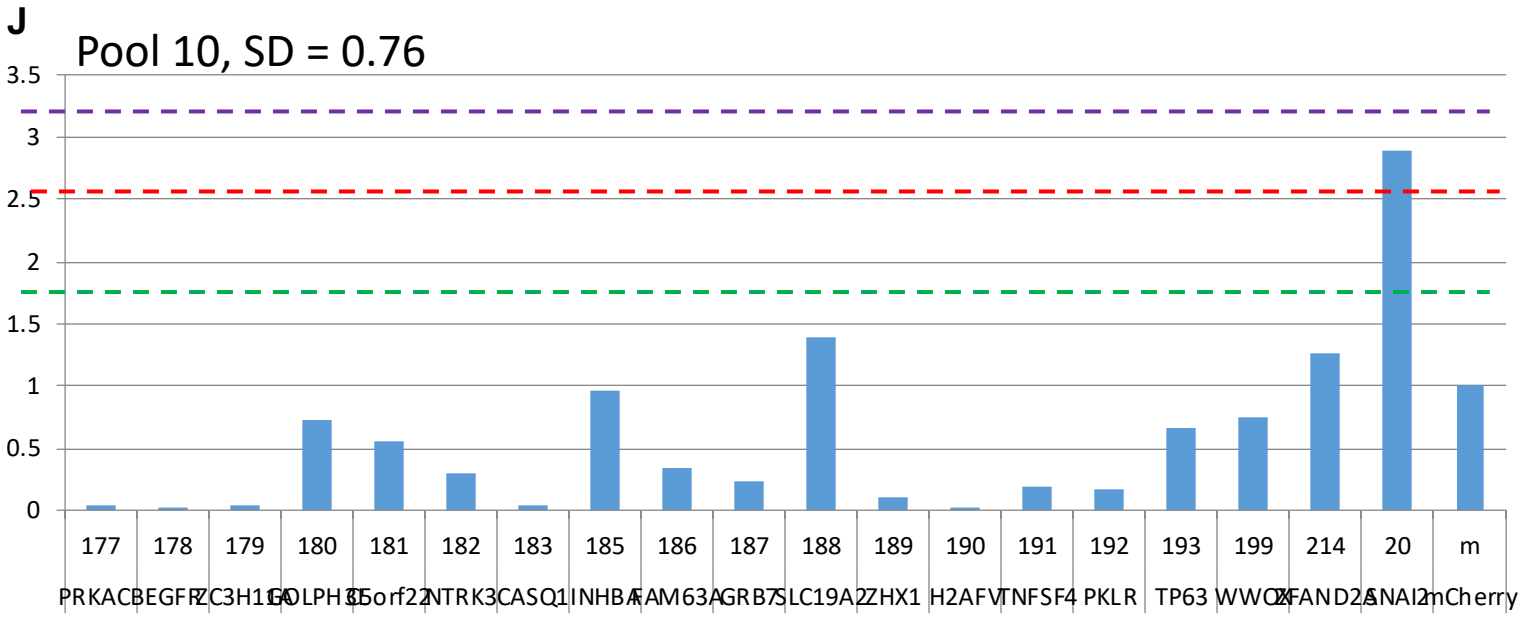


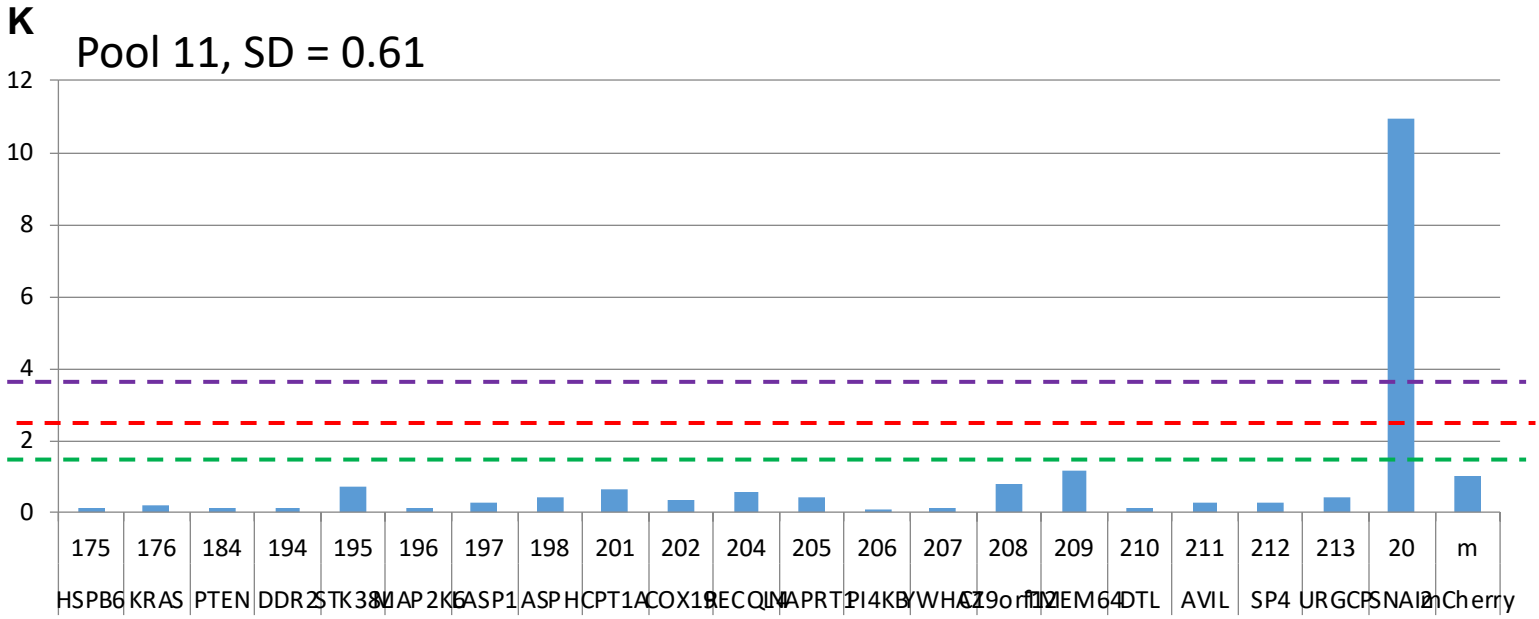


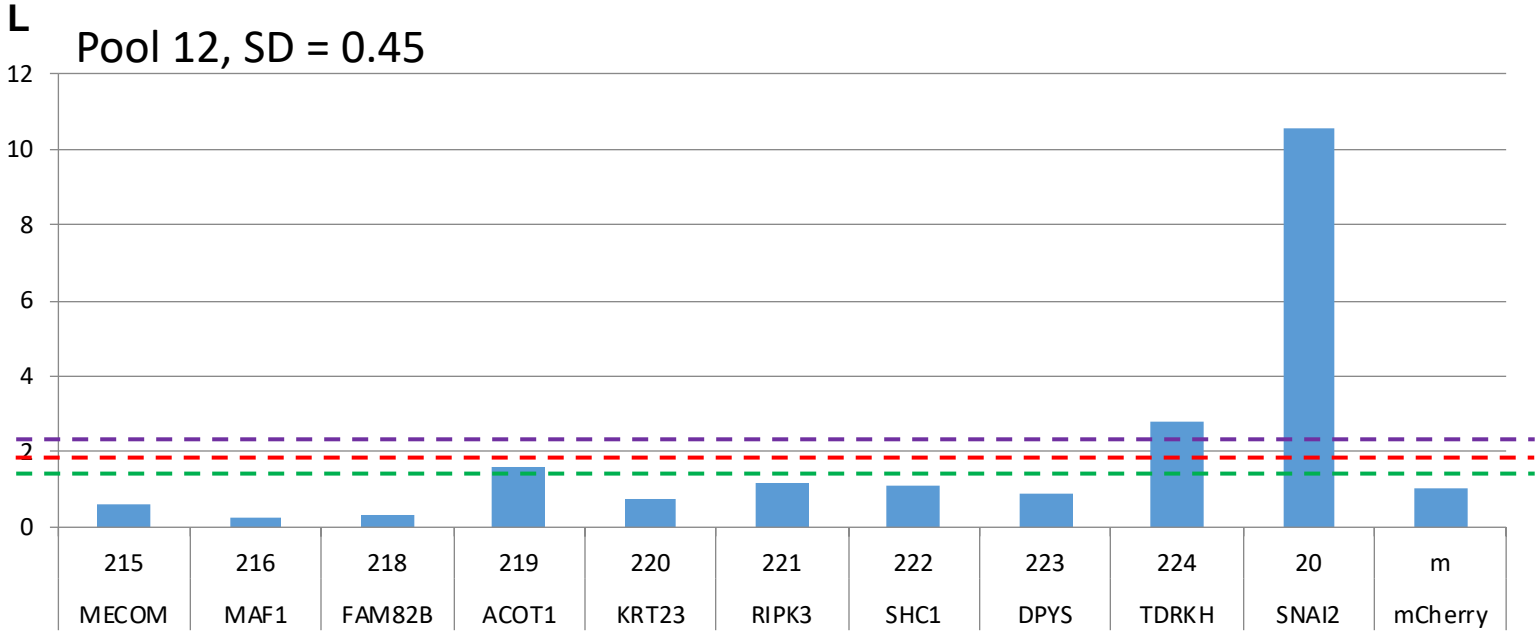

**Figure S1 A-L Fold change invasion for candidate genes from individual groups relative to mCherry of the respective cohort.** Hits within individual groups were pooled and their fold change invasion was calculated relative to the negative control, mCherry, of the corresponding cohort. Standard deviation (SD) (green dashed line), 2X SD (red dashed line), and 3X SD (purple dashed line) was obtained across hits within each group. We identified hits that showed a fold-change invasion significantly higher than 3X SD of mCherry within the corresponding group.

# Supplemental Fig. 2

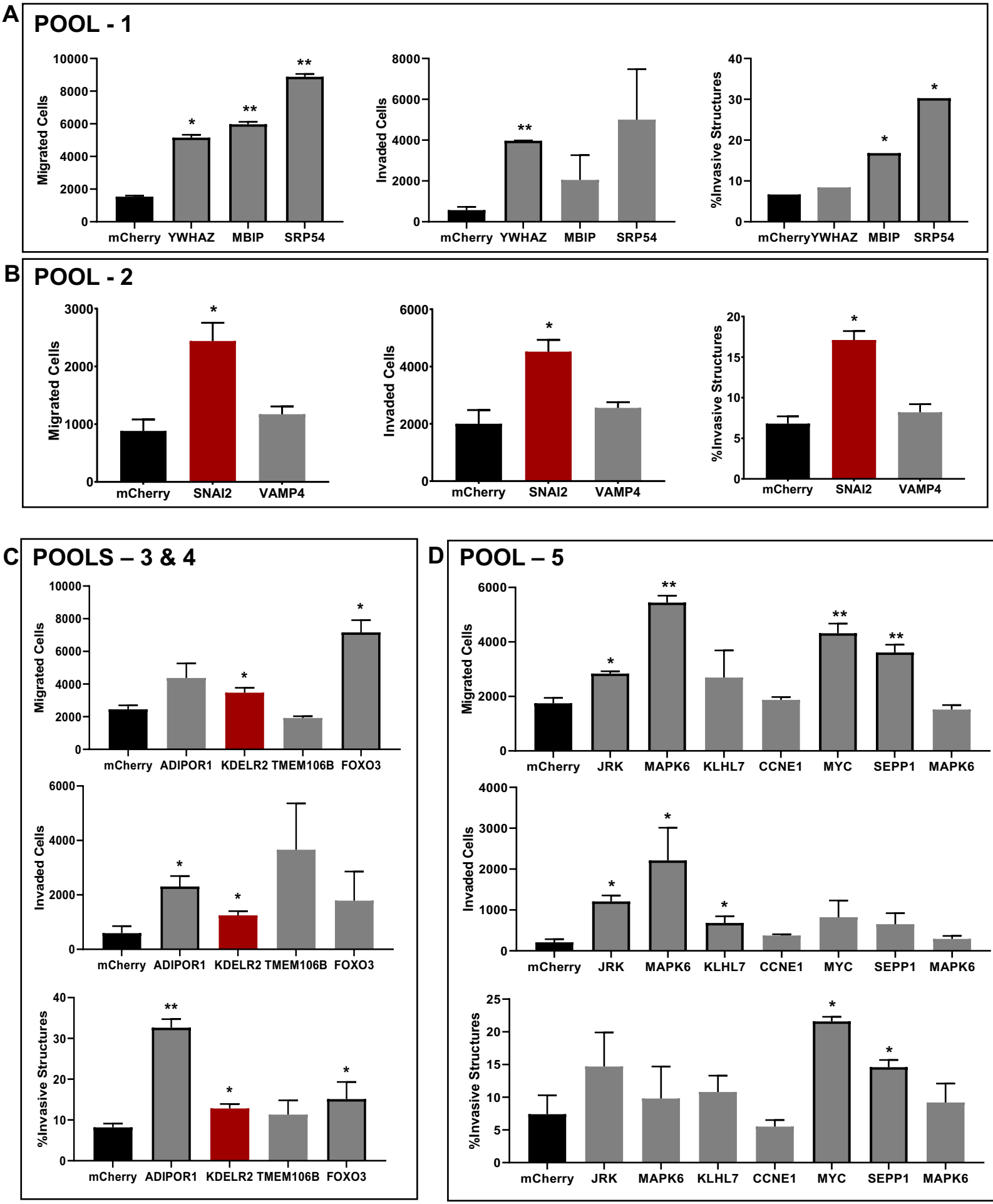

# Supplemental Fig. 2

**E**

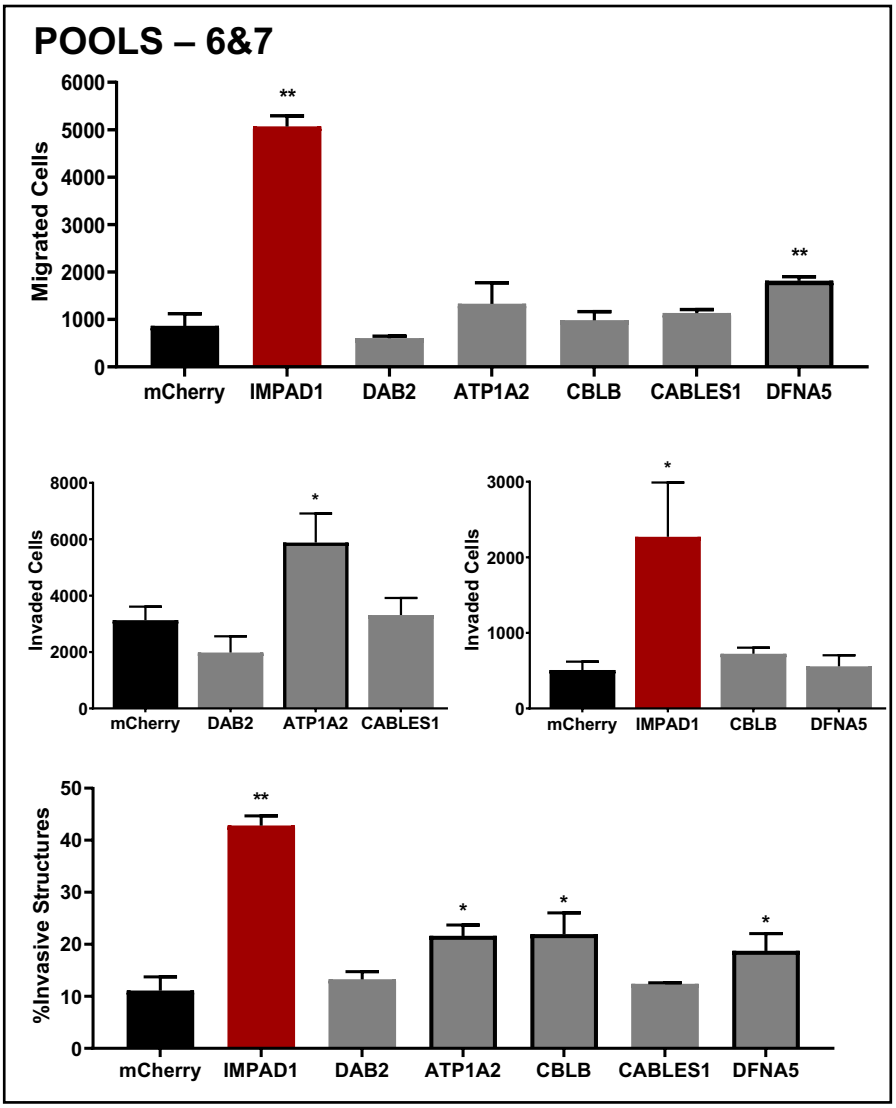


**F**

| HITS | MIGRATION | INVASION | 3D-INVASION | HITS | MIGRATION | INVASION | 3D-INVASION |
|---|---|---|---|---|---|---|---|
| YWHAZ | 0.007 | 0.0007 | 0.468 | KLHL7 | 0.239 | 0.022 | 0.133 |
| MBIP | 0.001 | 0.167 | 0.0447 | CCNE1 | 0.421 | 0.050 | 0.277 |
| SRP54 | 0.0007 | 0.089 | ---- | MYC | 0.001 | 0.117 | 0.001 |
| SNAI2 | 0.0036 | 0.002 | 0.00001 | SEPP1 | 0.001 | 0.093 | 0.011 |
| VAMP4 | 0.117 | 0.173 | 0.146 | MAPK6 | 0.195 | 0.243 | 0.421 |
| ADIPOR1 | 0.056 | 0.005 | 0.0007 | IMPAD1 | 0.001 | 0.048 | 0.0000006 |
| KDELR2 | 0.011 | 0.028 | 0.004 | DAB2 | 0.075 | 0.832 | 0.330 |
| TMEM106B | 0.043 | 0.086 | 0.232 | ATP1A2 | 0.279 | 0.009 | 0.002 |
| FOXO3 | 0.0048 | 0.187 | 0.039 | CBLB | 0.210 | 0.059 | 0.008 |
| JRK | 0.005 | 0.002 | 0.062 | CABLES1 | 0.074 | 0.085 | 0.540 |
| MAPK6 | 0.0001 | 0.048 | 0.449 | DFNA5 | 0.0002 | 0.669 | 0.010 |

**Figure S2 A-F Validation of hits from individual groups by using 2D migration and invasion, and 3D invasion identifies SNAI2, IMPAD1, and KDELR2 as drivers of invasion. A-E** The hits that demonstrated a fold-change invasion significantly higher than 3X SD in Fig S1 were validated by using 2D migration and invasion, and 3D invasion assays. In addition to the positive control SNAI2, we identified IMPAD1 and KDELR2 as the only hits that showed a significant increase in invasion across all three assays (red bars). **F** P-values for all experiments in A-E was calculated by Student's T-test by using three experimental replicates. SNAI2, IMPAD1, and KDELR2 are the only three hits showing p-value<0.05 across all three platforms (shown in blue).

# Supplemental Fig. 3

**A**

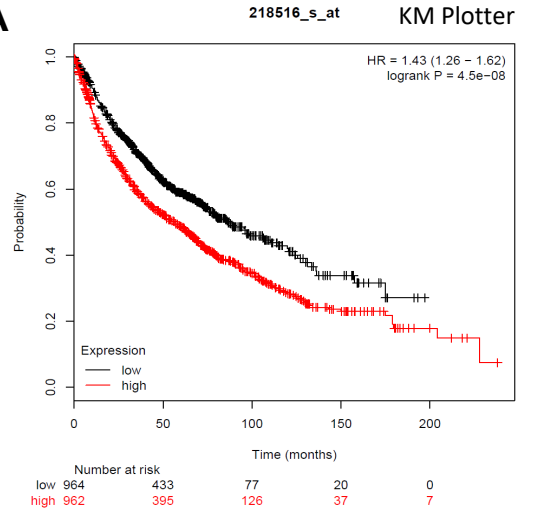


| Low Expression (months) | High Expression (months) |
|---|---|
| 86.27 | 56.8 |

**B**

Lung Adenocarcinoma –
Human Protein Atlas Dataset

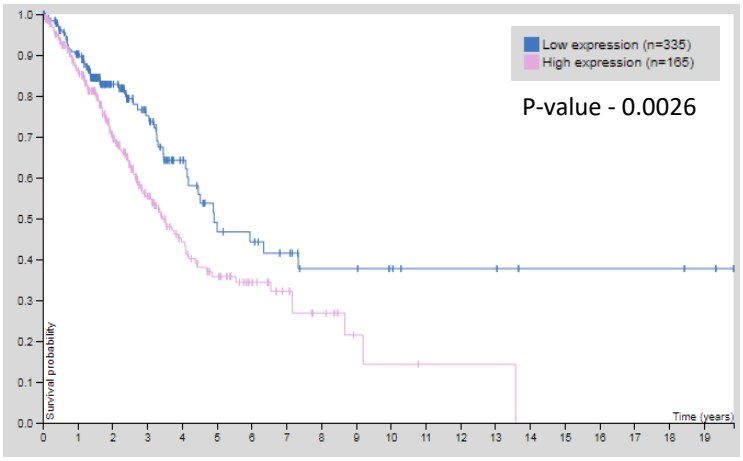


| 5-year survival low | 5-year survival high |
|---|---|
| 49% | 36% |

**C**

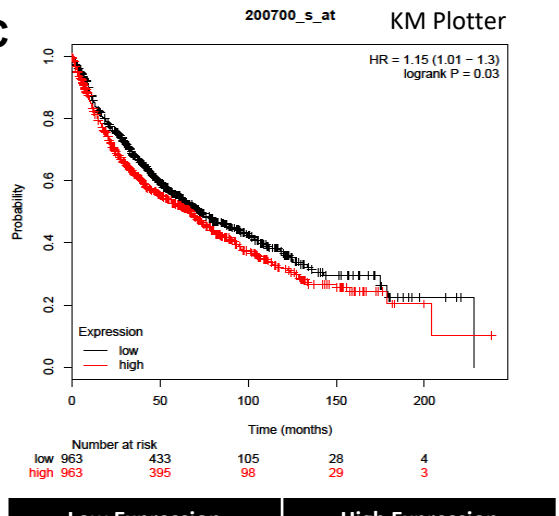


| Low Expression (months) | High Expression (months) |
|---|---|
| 72.33 | 67 |

**D**

Lung Adenocarcinoma –
Human Protein Atlas Dataset

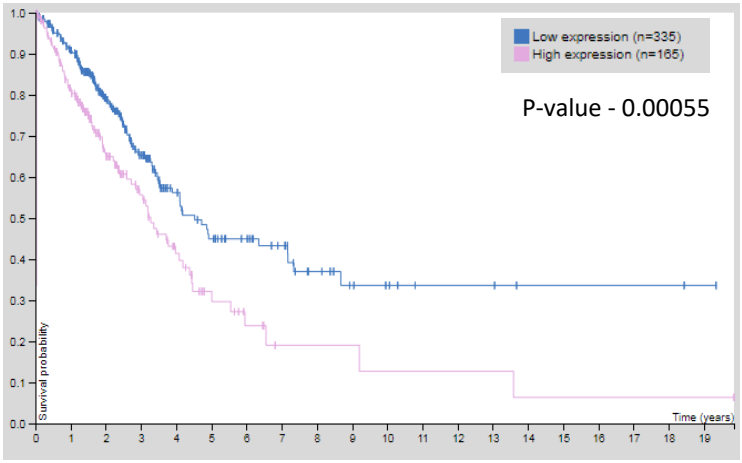


| 5-year survival low | 5-year survival high |
|---|---|
| 45% | 32% |

**E**

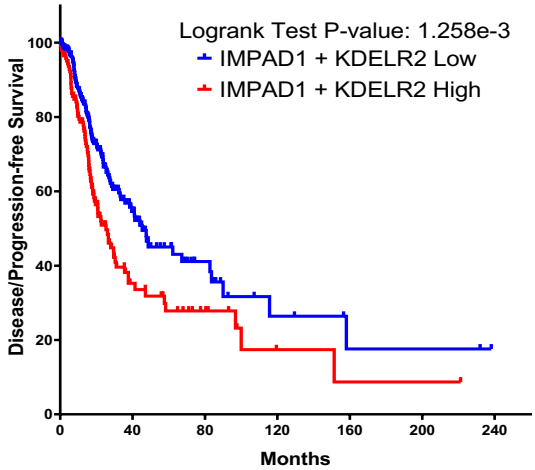


cBioportal

| Low Expression (months) | High Expression (months) |
|---|---|
| 45.27 | 25.33 |

# Supplemental Fig. 3

**F**

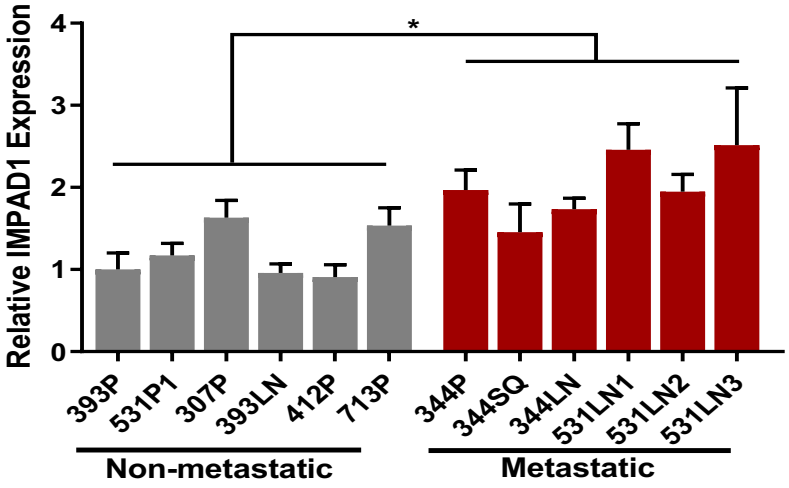


**G**

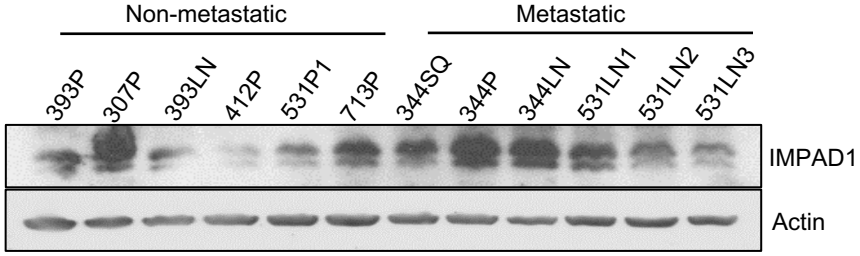


**H**

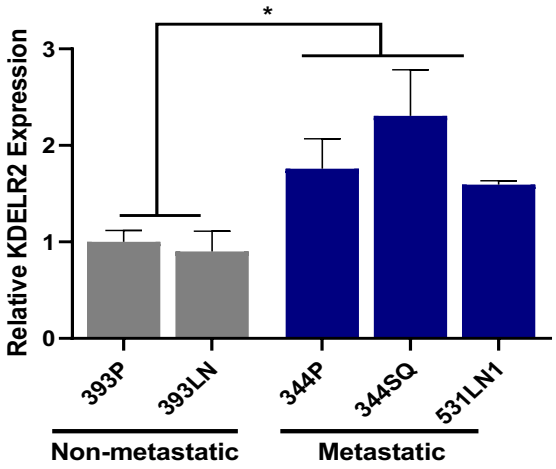


**I**

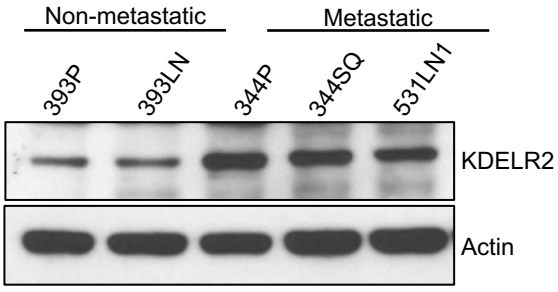

**Figure S3 IMPAD1 and KDELR2 amplification correlates with significantly worse disease-free survival. A, B** High IMPAD1 mRNA (A – KM Plotter) and protein (B – Human Protein Atlas Dataset) expression shows a worse disease-free survival compared to low IMPAD1 expression. **C, D** High KDELR2 mRNA (C – KM Plotter) and protein (D – Human Protein Atlas Dataset) expression shows a worse disease-free survival compared to low KDELR2 expression. **E** IMPAD1 and KDELR2 mRNA alterations demonstrate worse disease-free survival as compared to samples with no alterations. Median survival is mentioned in the tables below each graph. **F, G** Metastatic cells from KP murine cell panel show high IMPAD1 mRNA (F) and protein (G) expression compared to non-metastatic cells. **H, I** Metastatic cells from KP cell panel show high KDELR2 mRNA (H) and protein (I) expression compared to non-metastatic cells.

# Supplemental Fig. 4

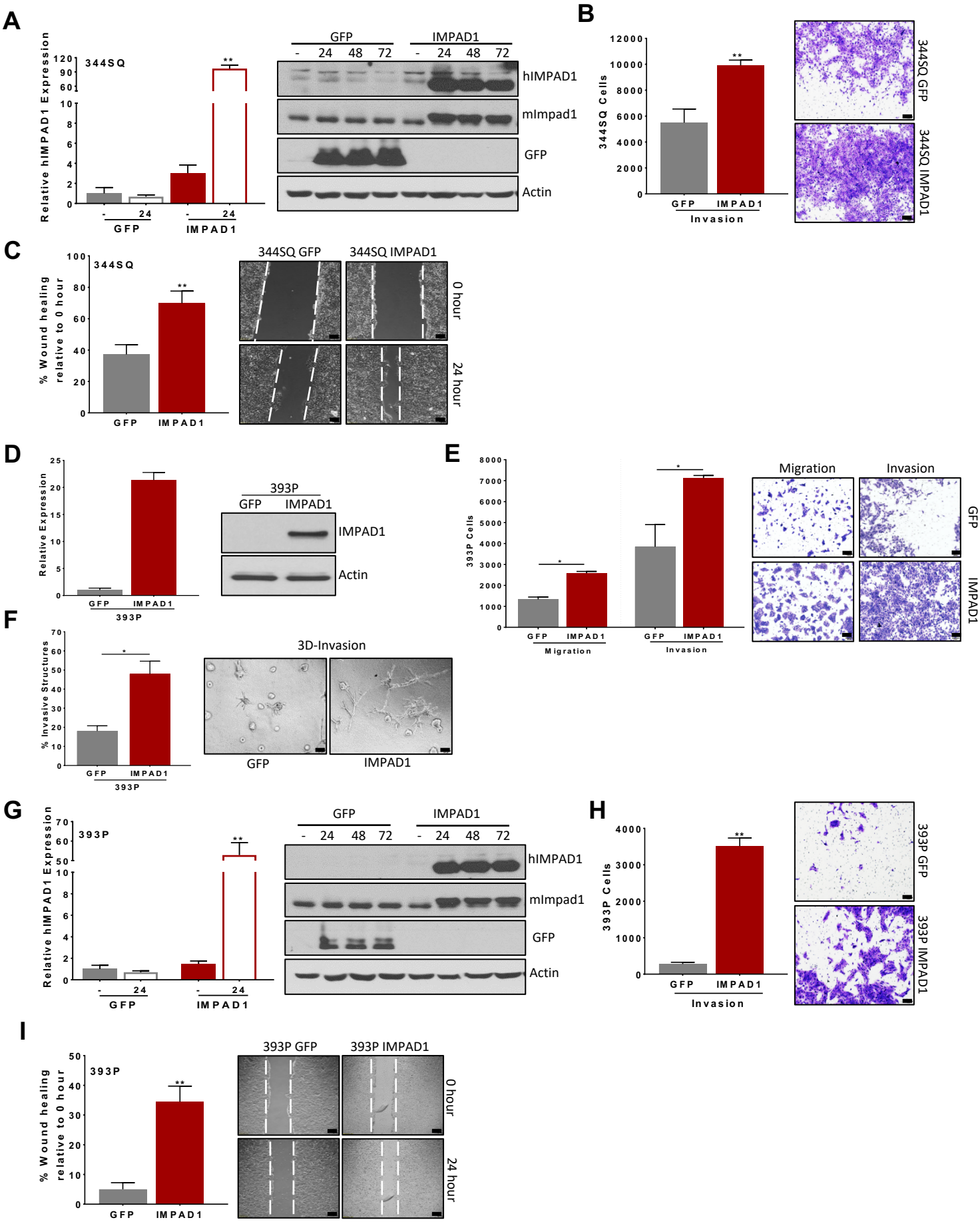

# Supplemental Fig. 4

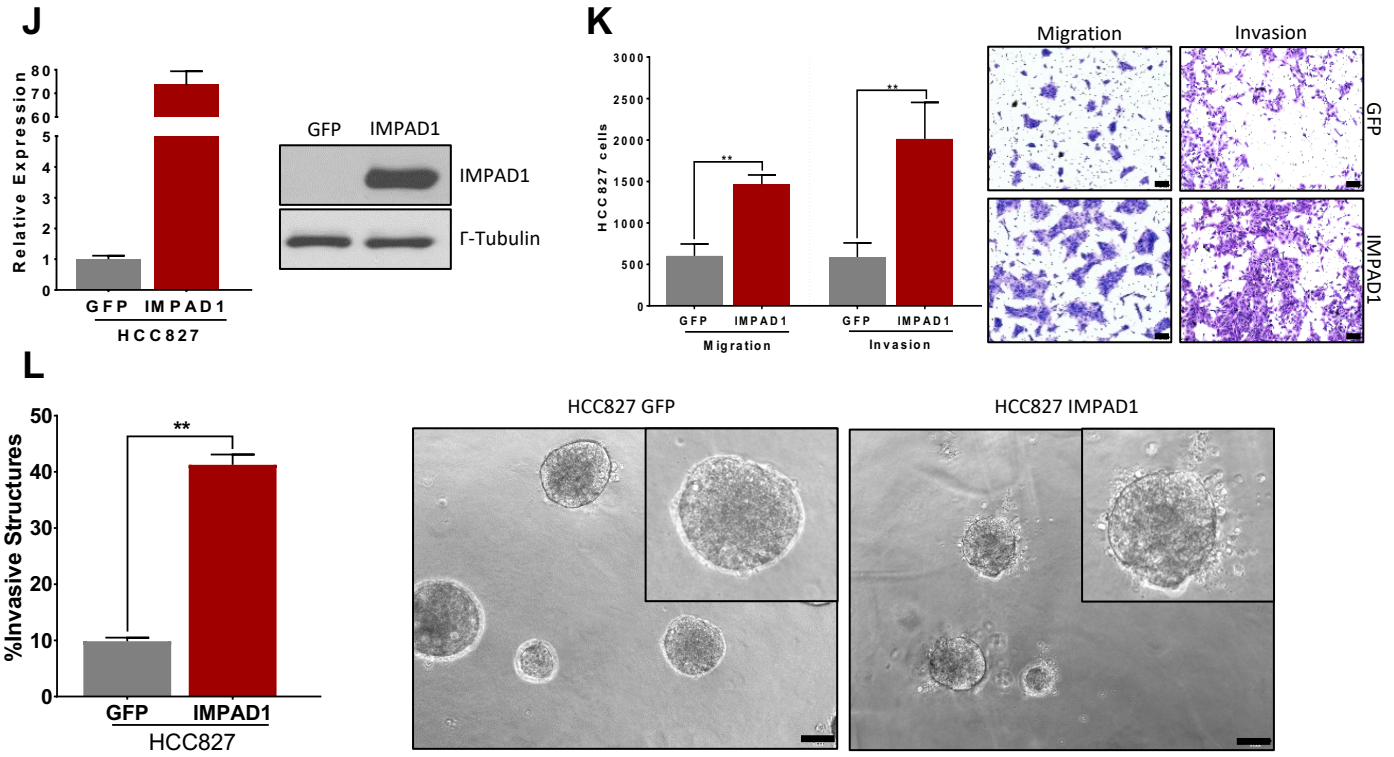


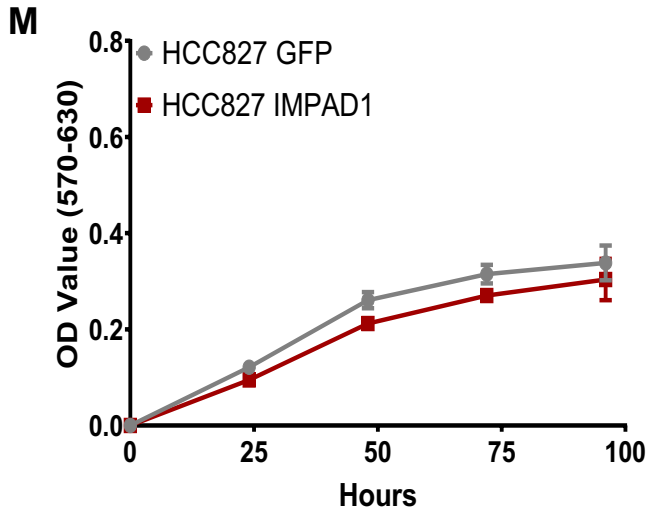


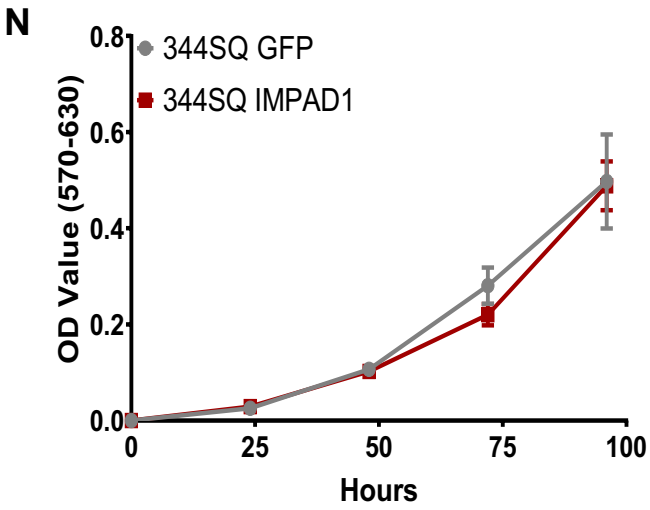


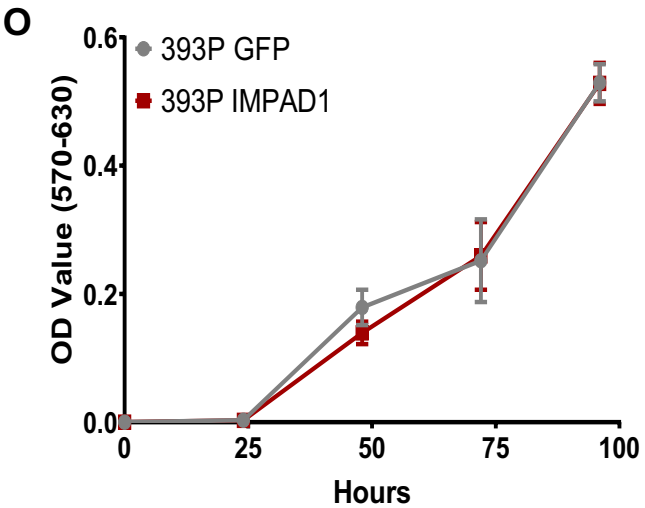


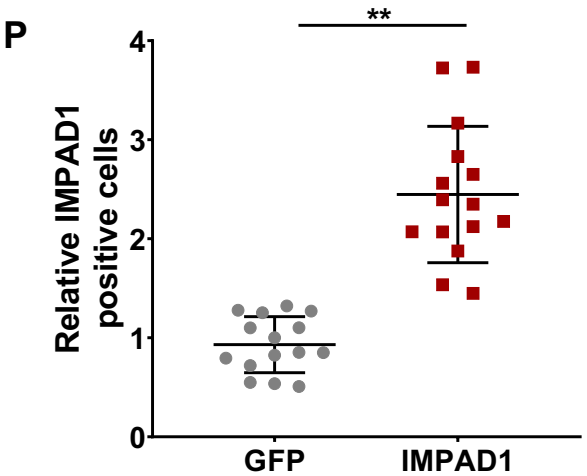

# Supplemental Fig. 4

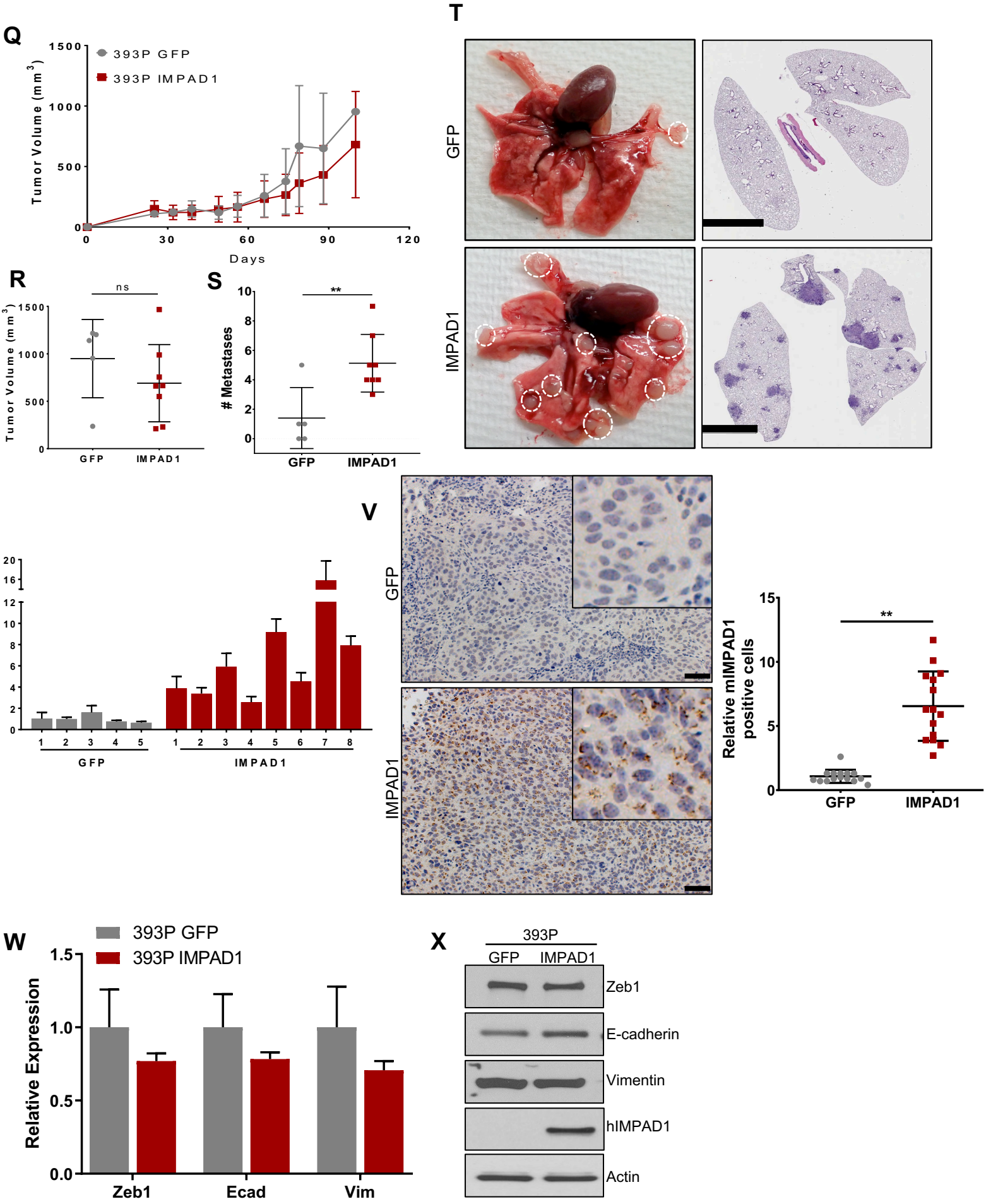

**Figure S4 IMPAD1 is sufficient to drive lung cancer invasion *in vitro* and metastasis *in vivo*. A** Doxycycline-inducible overexpression of human IMPAD1 in invasive 344SQ cells measured by RNA and protein. **B, C** IMPAD1 overexpression promotes cellular invasion by transwell assay (scale bar: 100uM) (B) and motility by wound healing assay (scale bar: 200uM) (C) upon 24-hour induction. **D** Constitutive overexpression of human IMPAD1 in non-invasive 393P cells measured by RNA and protein. **E, F** IMPAD1 overexpression promotes 2D migration and invasion by transwell assays (E), as well as 3D invasion in collagen and matrigel (1.5 mg/ml) measured as % invasive structures (F) (scale bar: 100uM). **G** Doxycycline-inducible overexpression of human IMPAD1 in non-invasive 393P cells measured by RNA and protein. **H, I** IMPAD1 overexpression promotes cellular invasion by transwell assay (scale bar: 100uM) (H) and motility by wound healing assay (scale bar: 200uM) (I) upon 24-hour induction. **J** Constitutive overexpression of human IMPAD1 in non-invasive HCC827 cells measured by RNA and protein. **K, L** IMPAD1 overexpression promotes 2D migration and invasion by transwell assays (K), as well as 3D invasion in collagen and matrigel (1.5 mg/ml) measured as % invasive structures (L) (scale bar: 100uM). **M-O** IMPAD1 overexpression does not alter cellular proliferation *in vitro* as demonstrated by MTT assay and measured by the OD value in HCC827 (M), 344SQ (N), and 393P (O) cells. **P** 344SQ IMPAD1 primary tumors show IMPAD1 overexpression compared to GFP control by IHC as quantified here. **Q, R** Primary tumor growth for non-metastatic 393P GFP and IMPAD1 overexpressing cells injected subcutaneously into mice (Q) over time, and (R) at time of euthanasia. **S** IMPAD1 overexpressing cells form significantly more lung metastatic nodules compared to GFP control. **T** Representative lungs and their respective H&E sections showing increased metastases in lungs from mice injected with IMPAD1 overexpressing cells compared to control (scale bar: 5mM). **U, V** Analysis to confirm overexpression of IMPAD1 in syngeneic tumors by (U) qPCR for RNA, and (V) IHC for protein also showing quantification (scale bar: 50uM). **W, X** IMPAD1 expression does not alter EMT status of cancer cells as depicted by no change in mRNA (W) or protein (X) levels of EMT markers upon IMPAD1 overexpression in epithelial 393P cells. EMT markers were probed on the same blots as in Fig. 2A and IMPAD1 and Actin blots are re-shown here.

# Supplemental Fig. 5

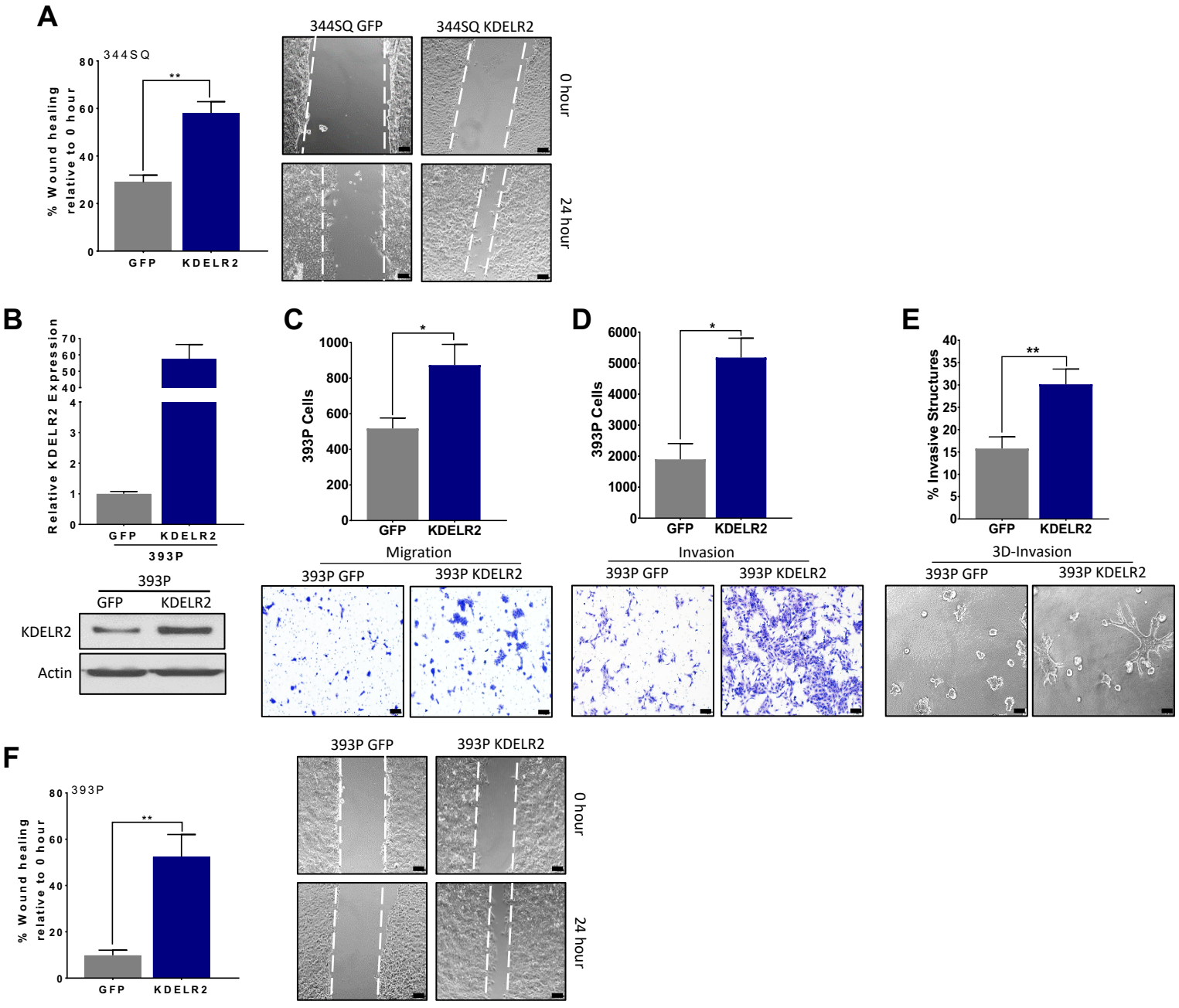

# Supplemental Fig. 5

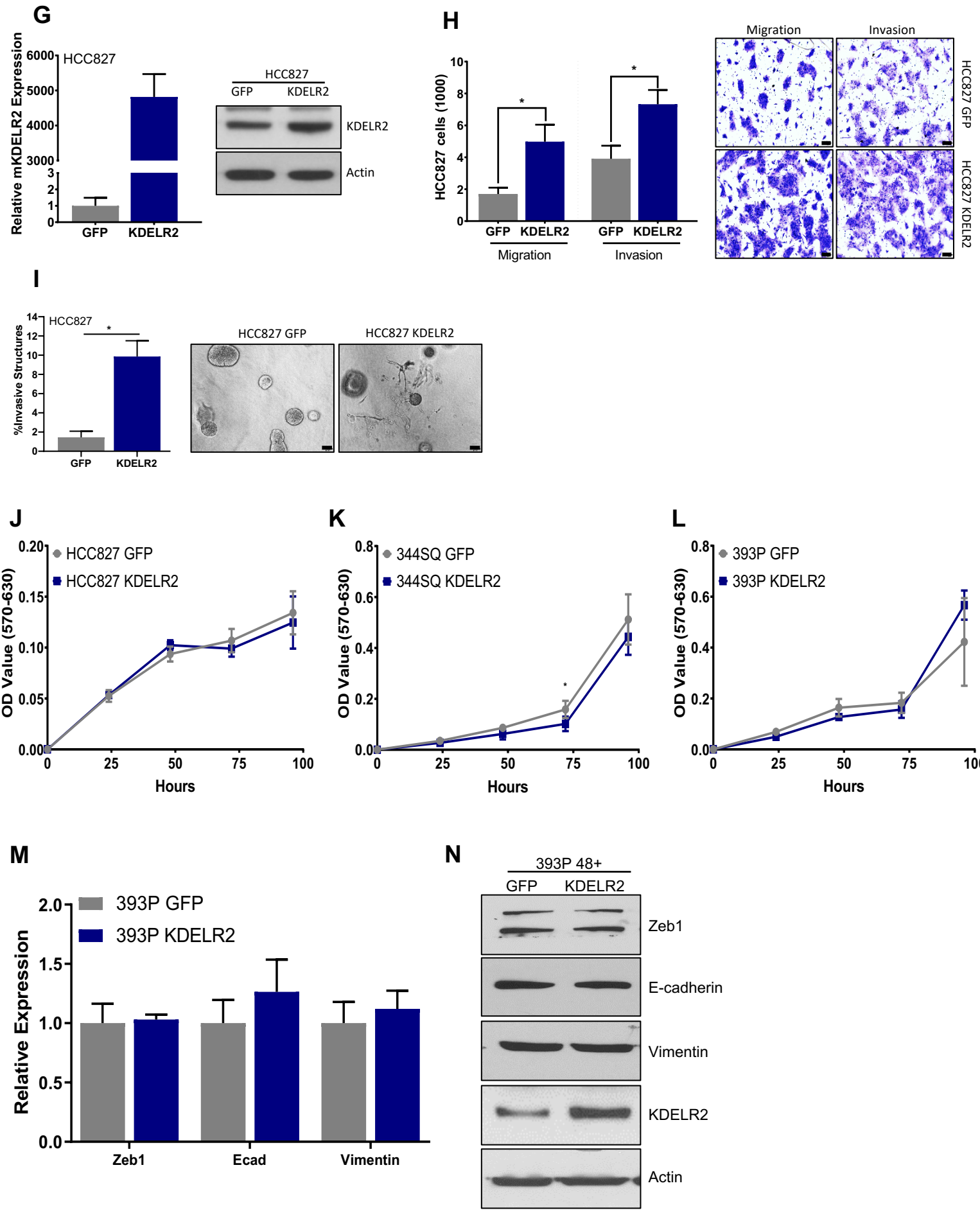

**Figure S5 KDELR2 is sufficient to drive lung cancer invasion *in vitro* and metastasis *in vivo*.** **A** KDELR2 overexpression promotes cellular motility by wound healing assay upon 24-hour induction (scale bar: 200uM). **B** Doxycycline-inducible overexpression of mouse KDELR2 in non-invasive 393P cells measured by RNA and protein. **C-F** KDELR2 overexpression promotes 2D migration (C) and invasion (D) by transwell assay, 3D invasion in collagen and matrigel (1.5 mg/ml) measured as % invasive structures (E), and cellular motility by wound healing assay (scale bar: 200uM) (F). **G** Doxycycline-inducible overexpression of mouse KDELR2 in non-invasive HCC827 cells measured by RNA and protein. **H, I** KDELR2 overexpression promotes 2D migration and invasion by transwell assays (H), as well as 3D invasion in collagen and matrigel (1.5 mg/ml) measured as % invasive structures (I). **J-L** KDELR2 overexpression does not alter cellular proliferation *in vitro* as demonstrated by MTT assay and measured by the OD value in HCC827 (J), 344SQ (K), and 393P (L) cells. All images other than wound healing assays have scale bars: 100uM. **M, N** KDELR2 expression does not alter EMT status of cancer cells as depicted by no change in mRNA (M) or protein (N) levels of EMT markers upon 48-hour doxycycline induction of KDELR2 in epithelial 393P cells. EMT markers were probed on the same blots as in Fig. 3A and KDELR2 and Actin blots are re-shown here.

# Supplemental Fig. 6

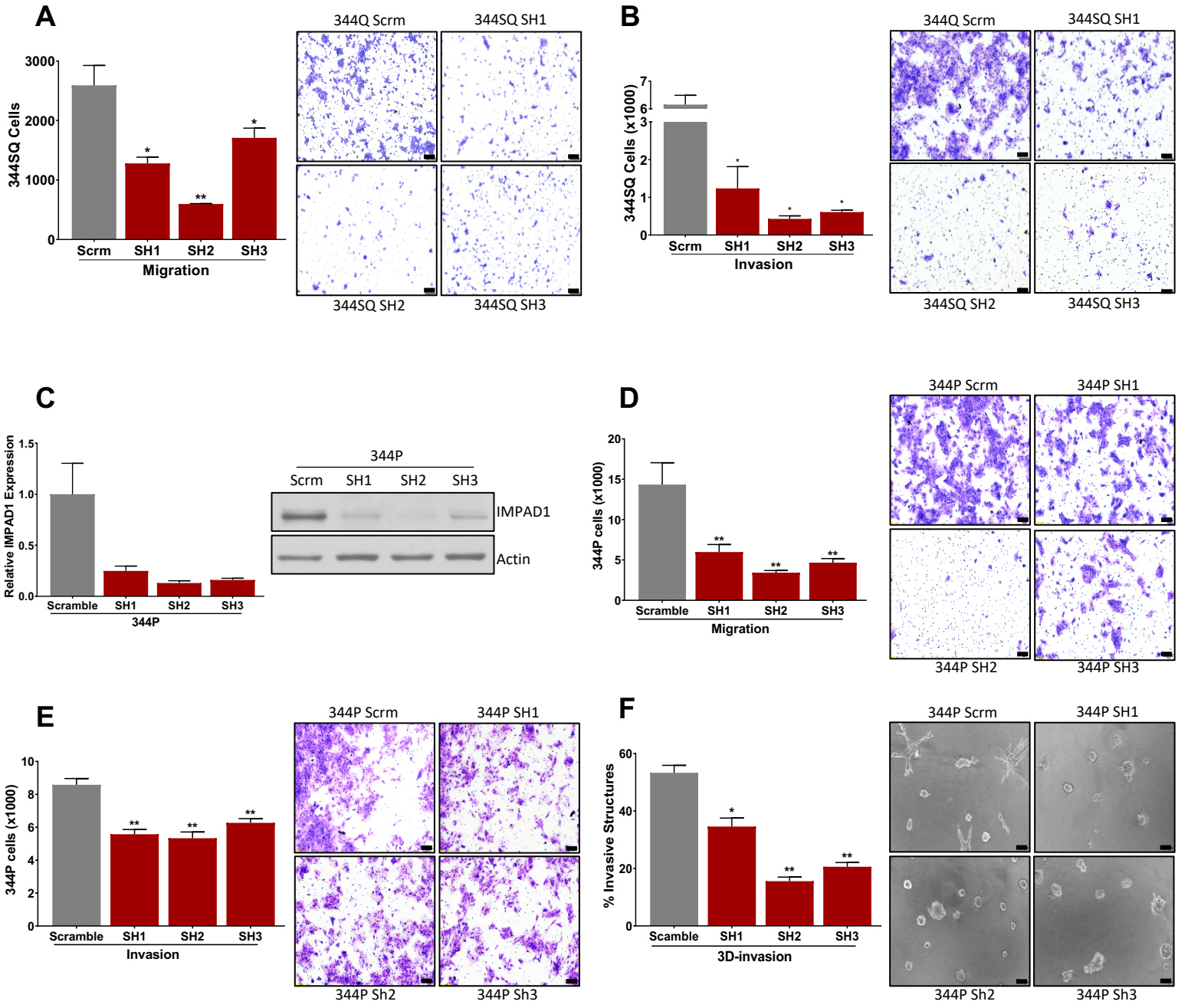

# Supplemental Fig. 6

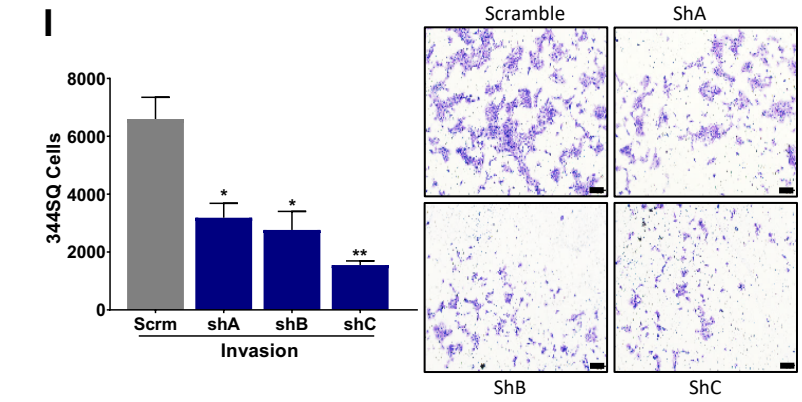


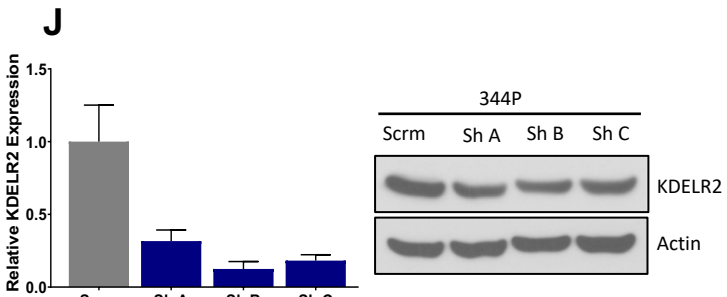


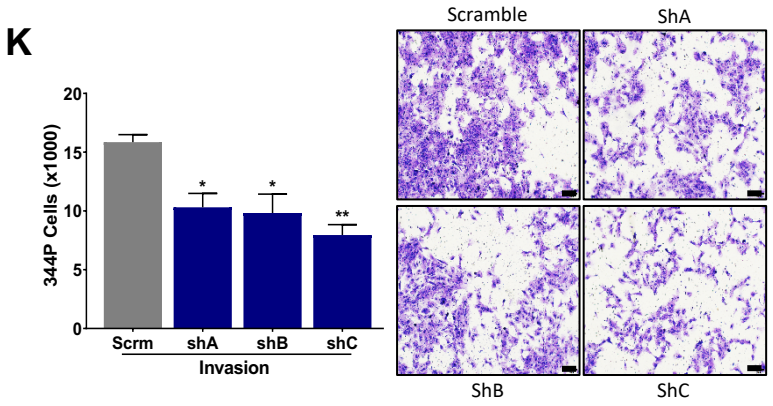


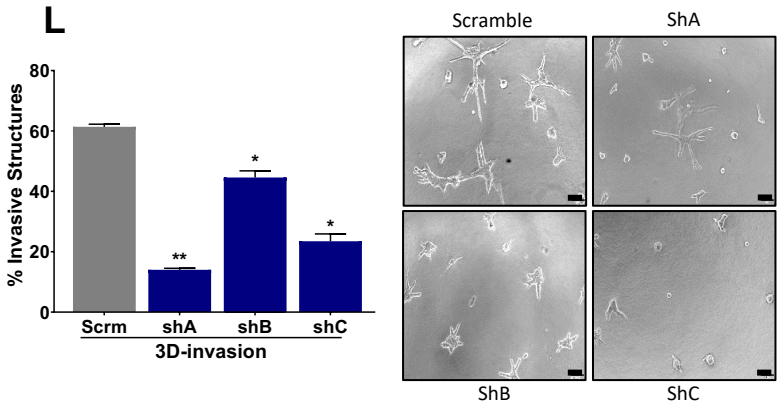


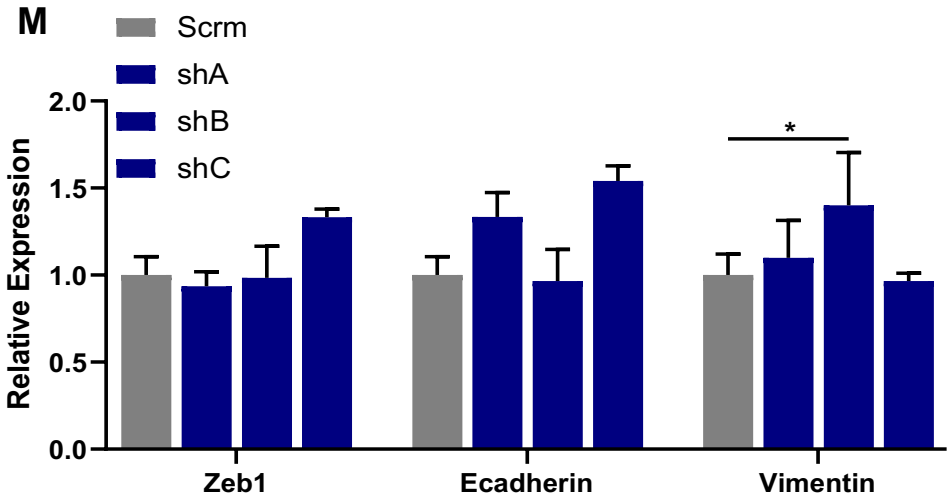


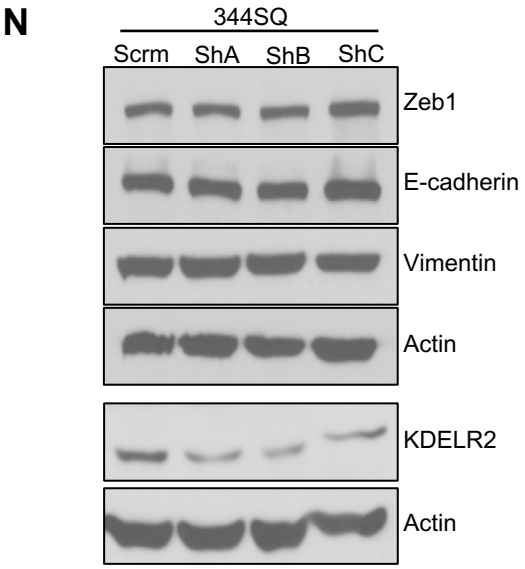

**Figure S6 IMPAD1 or KDELR2 expression is necessary for invasive ability of lung cancer cells. A, B** Knockdown of IMPAD1 with 3 different shRNAs show a significant decrease in 2D migration (A) and invasion (B) of 344SQ cells as compared to scramble. **C** IMPAD1 repression by SH1, SH2, and SH3 shRNAs in another metastatic KP cell line, 344P, measured by RNA and protein. **D, E** Knockdown of IMPAD1 in 344P cells show a significant decrease in migration (D) and invasion (E) as compared to control. **F** IMPAD1 knockdown 344P cells form significantly less invasive structures compared to control in 3D matrix comprising of collagen and matrigel (1.5 mg/ml) by day 6. **G, H** IMPAD1 expression does not alter EMT status of cancer cells as depicted by no change in mRNA (G) or protein (H) levels of EMT markers upon knockdown of IMPAD1 in mesenchymal-like 344SQ cells. EMT markers were probed on the same blots as in Fig. 4A and IMPAD1 and Actin blots are re-shown here. **I** KDELR2 knockdown decreased invasion of 344SQ cells as compared to scramble control. **J** KDELR2 repression by shA, shB, and shC in another metastatic KP cell line, 344P, as measured by RNA and protein. **K** Knockdown of KDELR2 in 344P cells show a significant decrease in invasion as compared to scramble control. **L** KDELR2 knockdown 344P cells form significantly less invasive structures compared to scramble in 3D matrix comprising of collagen and matrigel (1.5 mg/ml) by day 6. All images have scale bars: 100uM. **M, N** KDELR2 expression does not alter EMT status of cancer cells as depicted by no change in mRNA (M) or protein (N) levels of EMT markers upon knockdown of KDELR2 in mesenchymal-like 344SQ cells. EMT markers and KDELR2 blots were run in parallel but on separate gels as KDELR2 is probed on PVDF whereas EMT markers are probed on nitrocellulose membrane. KDELR2 and Actin are the same as Fig. 4G.

# Supplemental Fig. 7

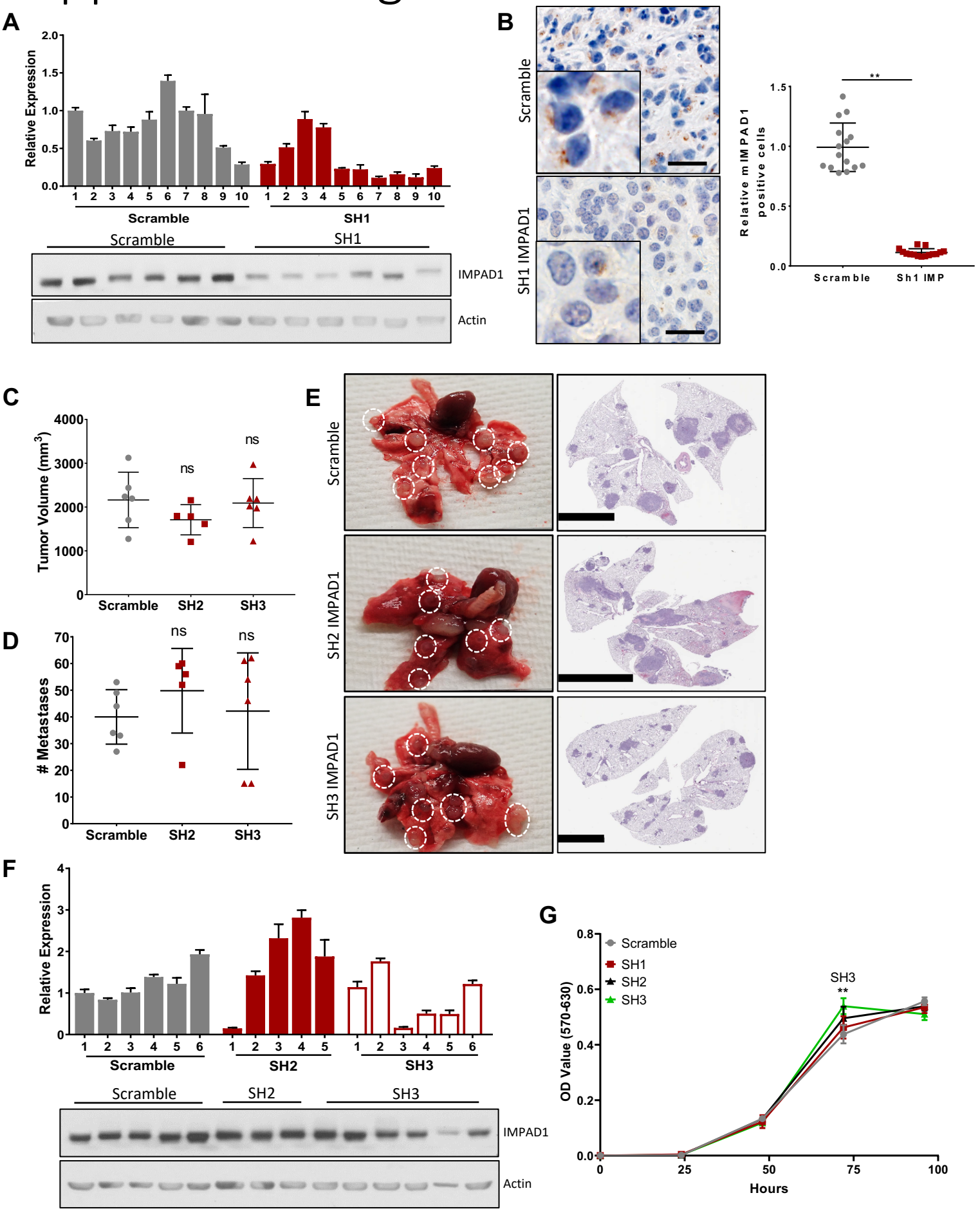

# Supplemental Fig. 7

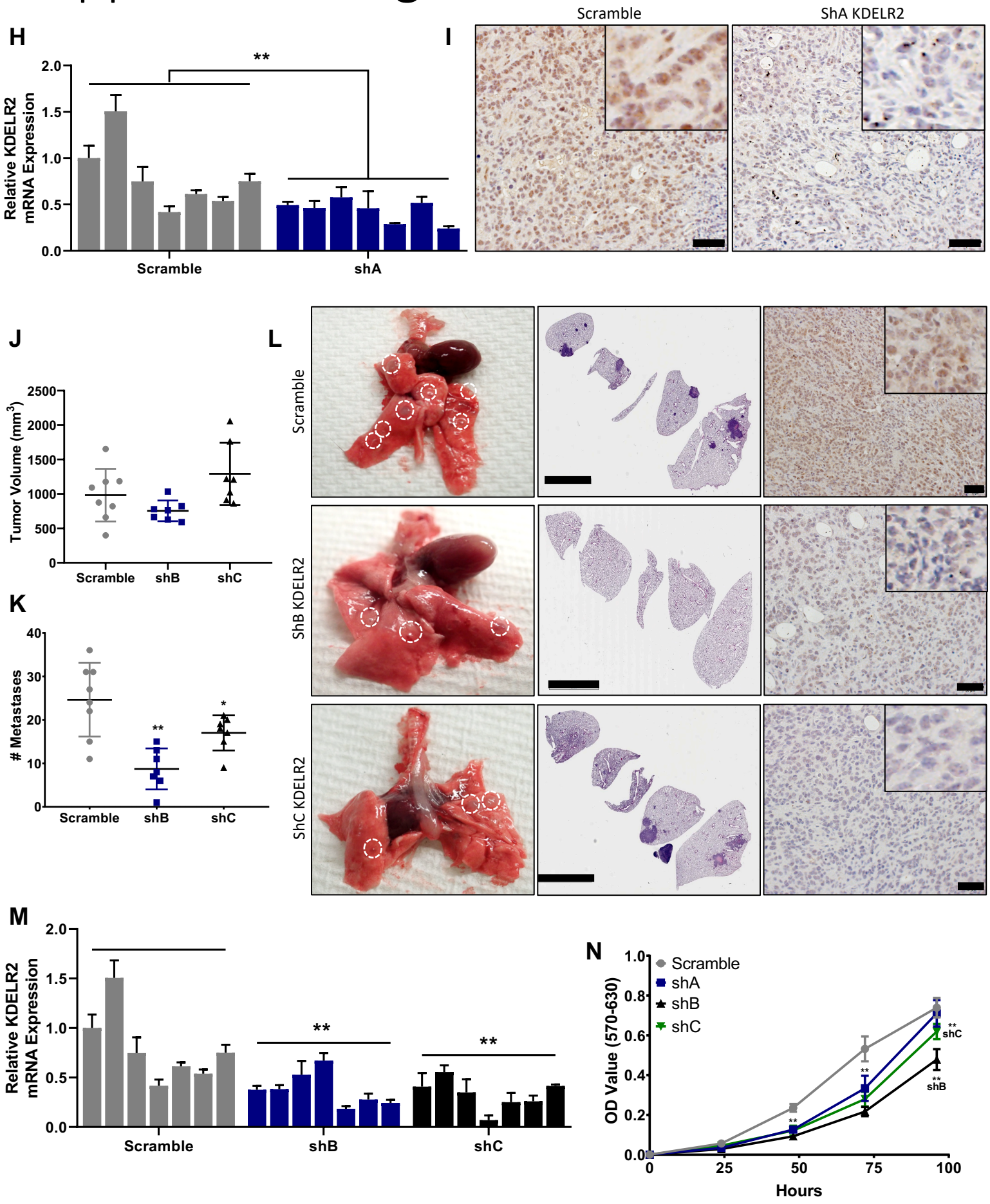

**Figure S7 IMPAD1 or KDELR2 expression is necessary for metastatic ability of lung cancer cells. A** Analysis of primary tumors to confirm knockdown of IMPAD1 by qPCR for RNA (upper), and western blot for protein (lower). **B** 344SQ SH1 IMPAD1 knockdown primary tumors show IMPAD1 repression by IHC (Scale bar: 20uM) as quantified. **C** Primary tumor growth at time of euthanasia for 344SQ scramble, and the other two shRNA knockdown cells (SH2 IMPAD1 and SH3 IMPAD1) injected subcutaneously into mice. **D** IMPAD1 knockdown cells show no change in lung metastatic nodules compared to scramble control. **E** Representative lungs and their respective H&E stained sections showing metastases in lungs from mice implanted with SH2 IMPAD1, and SH3 IMPAD1 cells compared to control (Scale bar: 5mM). **F** Analysis of primary tumors to ascertain knockdown of IMPAD1 by qPCR for RNA (upper), and western blot for protein (lower). **G** IMPAD1 knockdown does not alter cellular proliferation *in vitro* in 344SQ cells as demonstrated by the MTT assay. **H, I** Analysis of primary tumors to confirm knockdown of KDELR2 by qPCR for RNA (H), and IHC for protein (I) (Scale bar: 50uM). **J** Primary tumor growth at time of euthanasia for 344SQ scramble, and the other two shRNA knockdown cells (shB KDELR2 and shC KDELR2) implanted subcutaneously into mice. **K** KDELR2 knockdown tumors form significantly less lung metastatic nodules compared to scramble control. **L** Representative lungs and their respective H&E stained sections showing metastases in lungs from mice injected with shB KDELR2 and shC KDELR2 cells compared to control. KDELR2 staining of primary tumors by IHC confirms KDELR2 knockdown (Scale bar: 50uM). **M** Analysis of primary tumors to ascertain knockdown of KDELR2 by qPCR for RNA. **N** KDELR2 knockdown alters cellular proliferation *in vitro* in 344SQ cells as demonstrated by the MTT assay.

# Supplemental Fig. 8

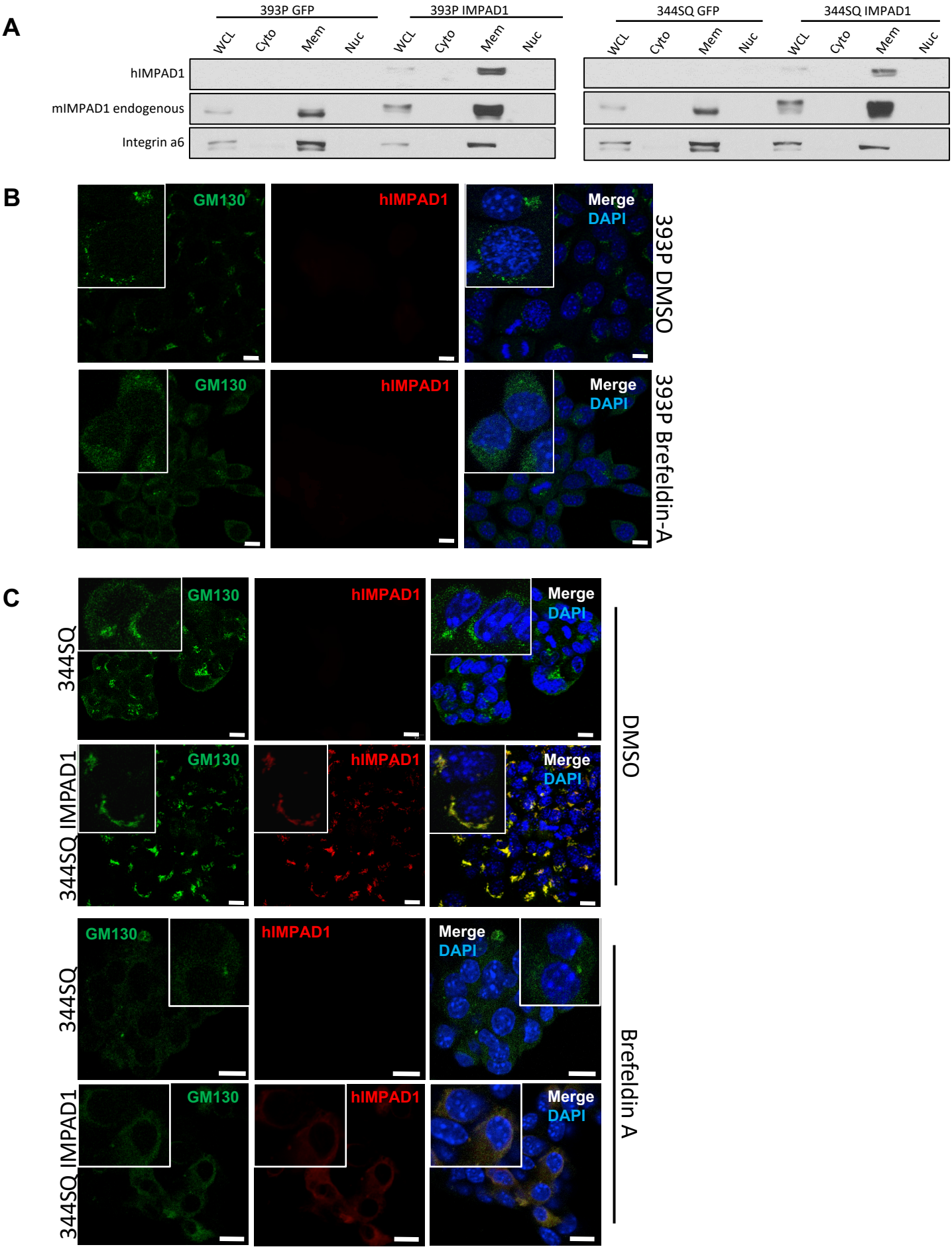

# Supplemental Fig. 8

**D**

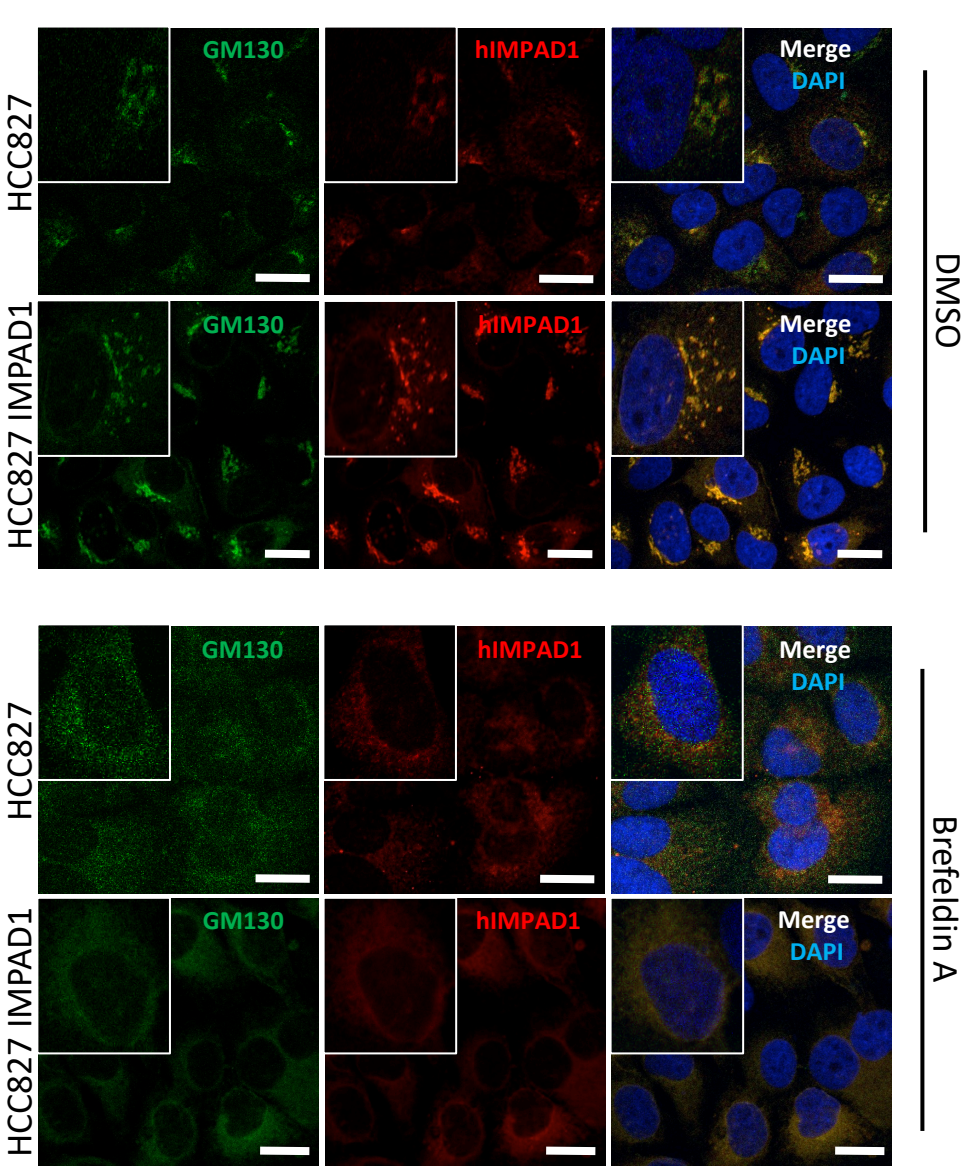

# Supplemental Fig. 8

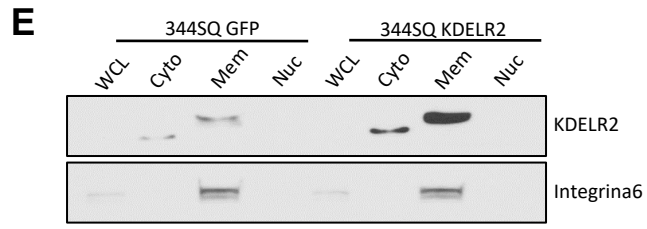


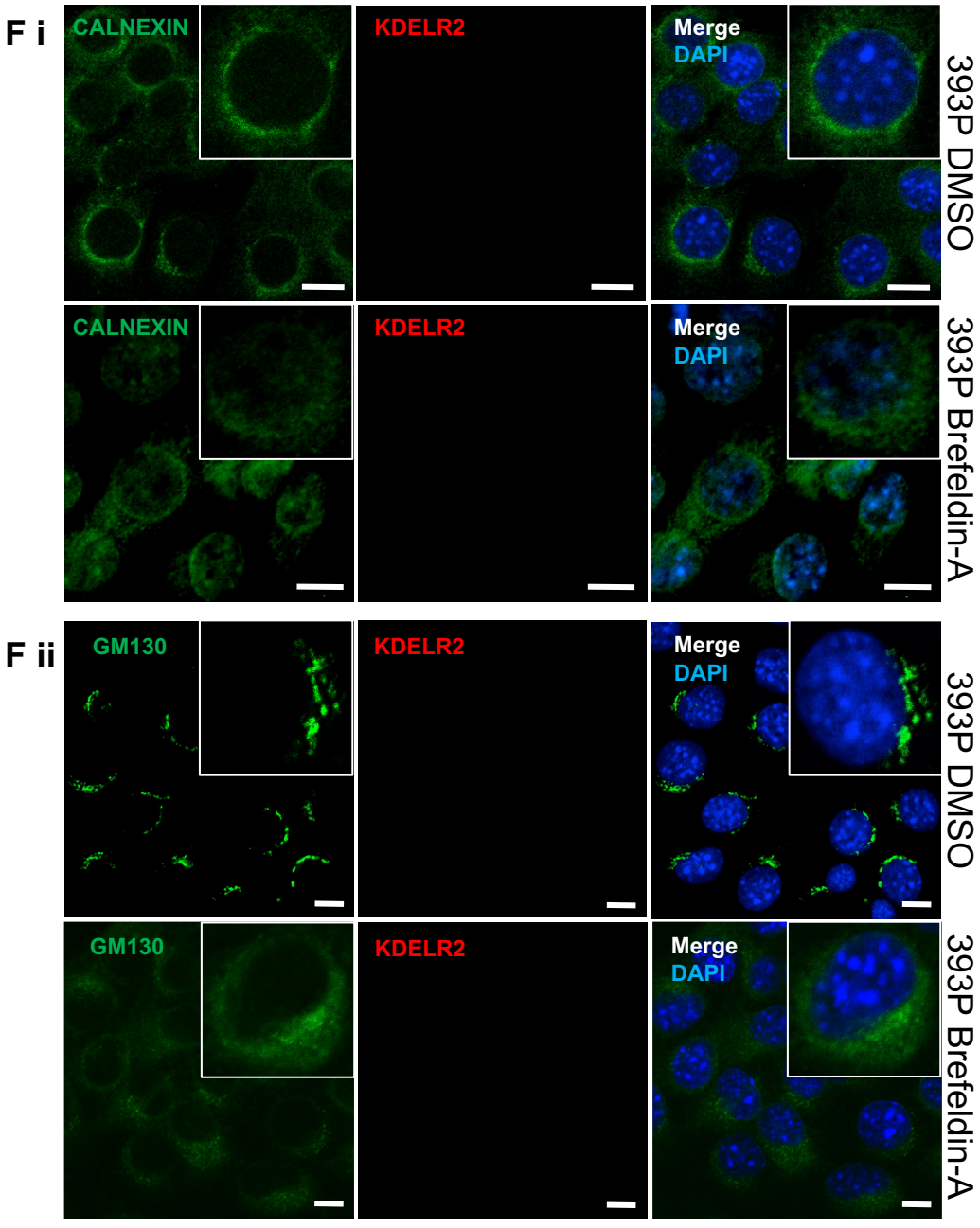

**Figure S8 IMPAD1 and KDELR2 localize to the Golgi-ER pathway. A** Fractionation assay with 393P and 344SQ cells overexpressing human IMPAD1 demonstrate that endogenous (mouse) and exogenous (human) IMPAD1 is primarily in the membrane fraction. Integrin α6 was used as the loading control for the membrane fraction. WCL – whole cell lysate, Cyto – cytoplasmic fraction, Mem – membrane fraction, Nuc – nuclear and cytoskeletal fraction. **B** Co-immunofluorescence with IMPAD1 (red) and Golgi marker, GM130 (green) in 393P control cells. Nucleus was counter-stained with DAPI. Cells were treated with DMSO (upper) or Brefeldin-A (1uM 6 hours) (lower). **C, D** Co-immunofluorescence with IMPAD1 (red) and Golgi marker, GM130 (green) in 344SQ (C) and HCC827 (D) cells with IMPAD1 overexpression or empty vector. Nucleus was stained with DAPI. Cells were treated with DMSO (upper) or Brefeldin-A (1uM 6 hours) (lower). **E** Fractionation assay with 344SQ cells expressing mouse KDELR2 demonstrate that KDELR2 is primarily in the membrane fraction. Integrin α6 was used as the loading control for the membrane fraction. WCL –whole cell lysate, Cyto – cytoplasmic fraction, Mem – membrane fraction, Nuc – nuclear and cytoskeletal fraction. Doxycycline induction – 48 hours. **F i, ii** Co-immunofluorescence with FLAG (red) and ER marker, Calnexin (green) (i) or FLAG (red) and Golgi marker, GM130 (green)(ii) in 393P control cells. Nucleus was stained with DAPI. Cells were treated with DMSO (upper) or Brefeldin-A (1uM 6 hours) (lower).

# Supplemental Fig. 9

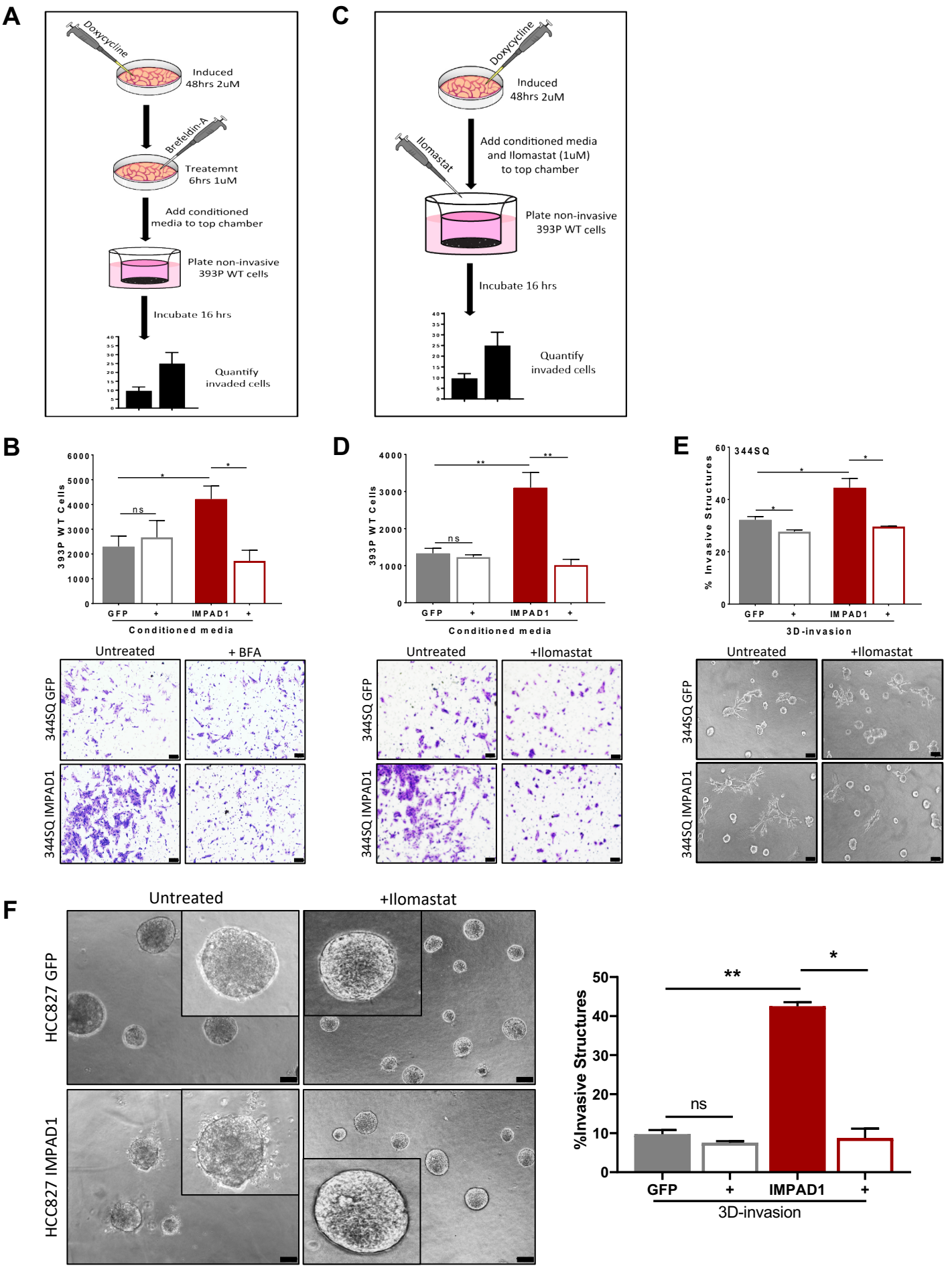

# Supplemental Fig. 9

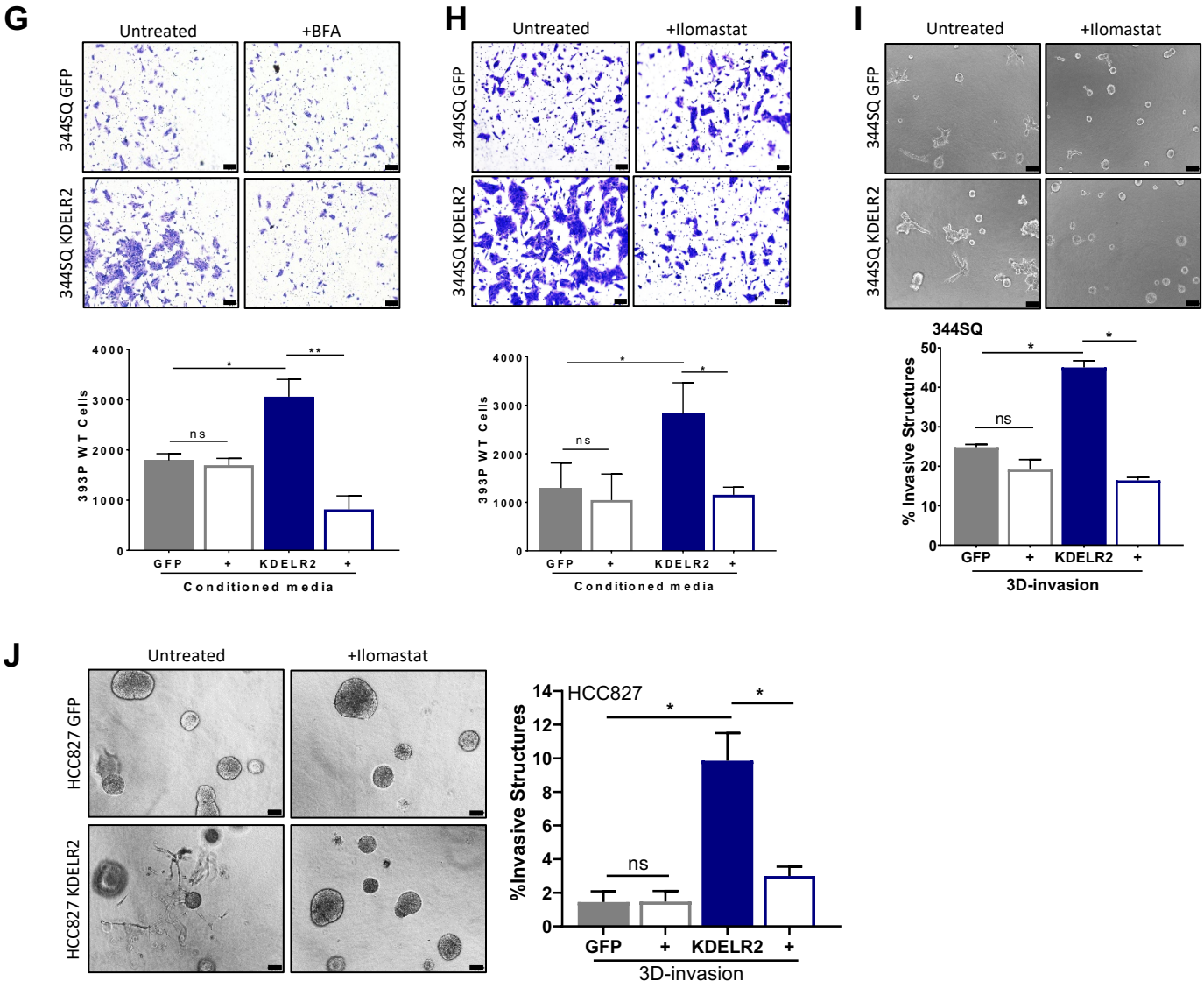

# Supplemental Fig. 9

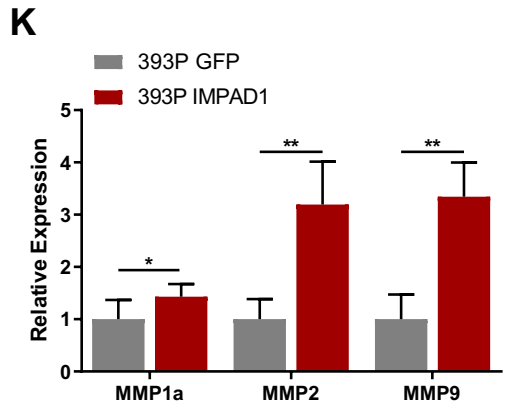


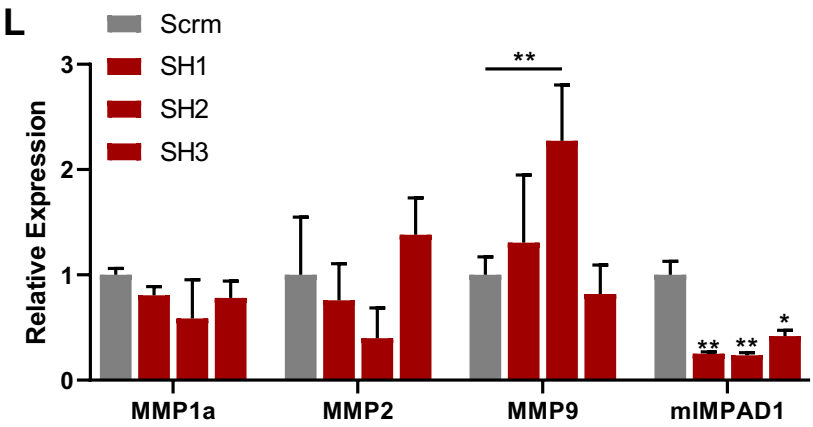


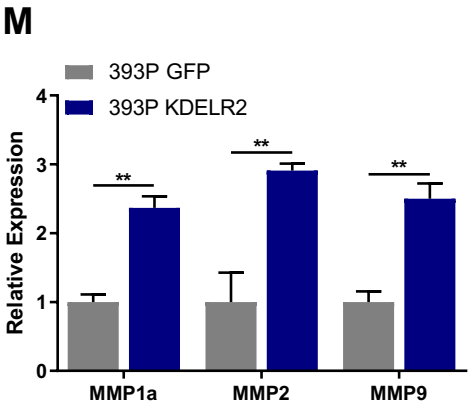


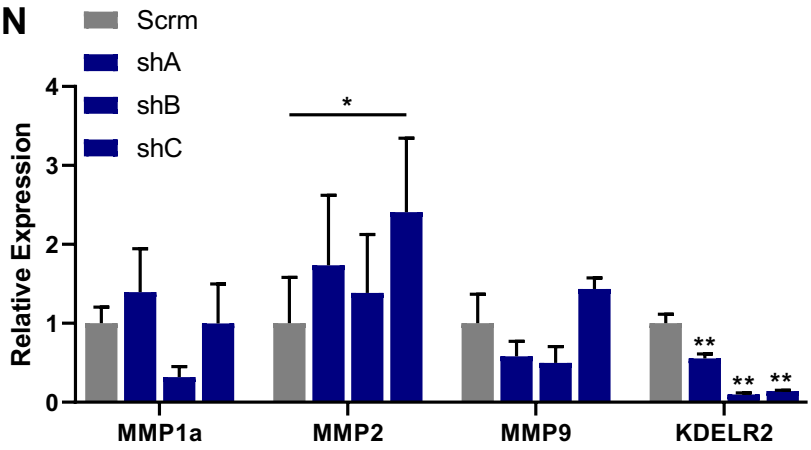


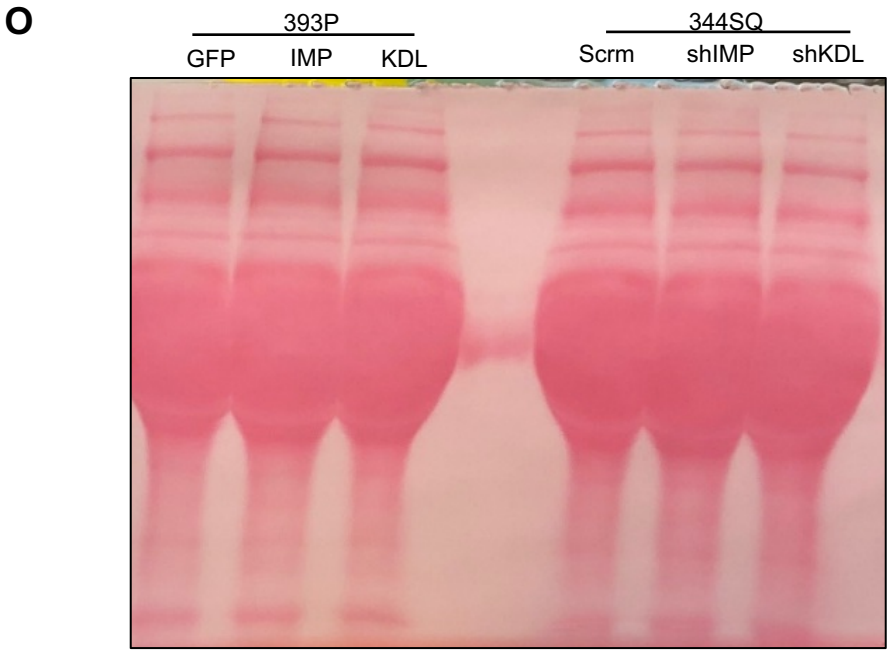

**Figure S9 IMPAD1 and KDELR2 independently regulate Golgi-mediated secretion of proteases such as MMPs to drive lung cancer invasion. A** Schematic workflow for secretome-mediated invasion assay – 24 hour-conditioned media (CM) was collected from cells that were doxycycline-induced for 48 hours. This CM with or without 6-hour BFA treatment was used to replenish the non-invasive parental 393P WT cells that were plated in Boyden chambers. After 16 hours of incubation, cells that invaded through the chambers were quantified to determine effect of the secretome on their invasiveness. **B** Number of 393P WT cells invaded were quantified, which shows that IMPAD1-mediated secretome is sufficient to drive invasion and this phenotype is repressed upon abrogating the Golgi with BFA (1uM 6 hours). **C** Schematic workflow for secretome-mediated invasion assay – 24 hour-conditioned media was collected from cells that were doxycycline-induced for 48 hours. This CM was used to replenish the non-invasive parental 393P WT cells that were plated in Boyden chambers. MMP inhibitor, Ilomastat 1uM, was added to the CM in the Boyden chamber. After 16 hours of incubation, cells that invaded were quantified to determine effect of the secretome on their invasiveness. **D** Number of 393P WT cells that invaded that were quantified, which shows that IMPAD1-mediated secretion of MMPs is sufficient to drive invasion. **E, F** Invasive structures formed upon IMPAD1 overexpression in collagen/matrigel matrix (1.5mg/ml) is inhibited upon MMP inhibition with Ilomastat (1uM) (day 5) in (E) mouse and (F) human cells. **G, H** Conditioned media from KDELR2 overexpressing cells induced for 48 hours is sufficient to promote invasiveness of 393P WT cells. This phenotype is reversed upon treatment with (G) BFA (1uM 6 hours), and (H) Ilomastat (1uM). **I, J** Invasive structures formed upon KDELR2 overexpression in collagen/matrigel matrix (1.5mg/ml) is inhibited upon MMP inhibition with Ilomastat (1uM) (day 5) in (I) mouse and (J) human cells. All images have scale bars: 100uM. **K** MMPs 1a, 2, and 9 upregulated upon 48 hours doxycycline-induced IMPAD1 expression in 393P cells. **L** No change in MMP mRNA levels upon IMPAD1 knockdown in 344SQ cells. **M** MMPs 1a, 2, and 9 upregulated upon doxycycline-induced KDELR2 expression at 48 hours in 393P cells. **N** No change in MMP mRNA levels upon KDELR2 knockdown in 344SQ cells. **O** Ponceau staining on blot run for CM collected from IMPAD1 and KDELR2 overexpressing and knockdown cells shows equal loading of the proteins.

# Supplemental Fig. 10

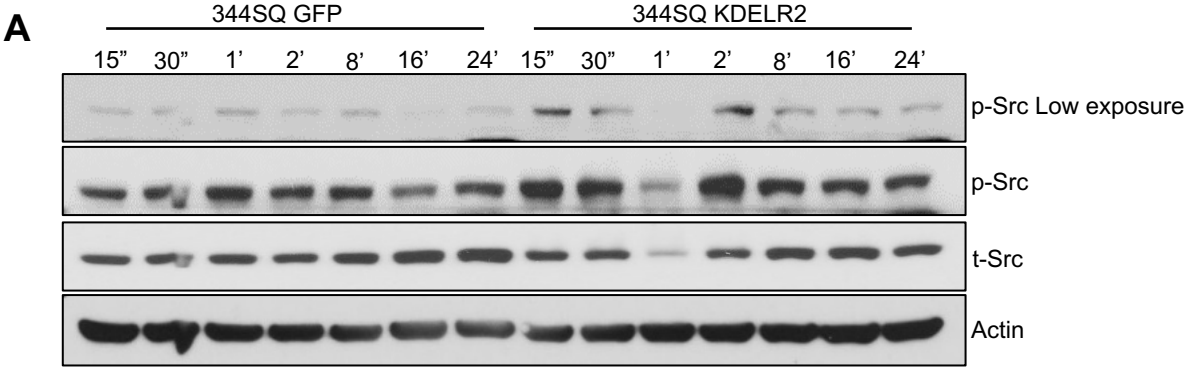


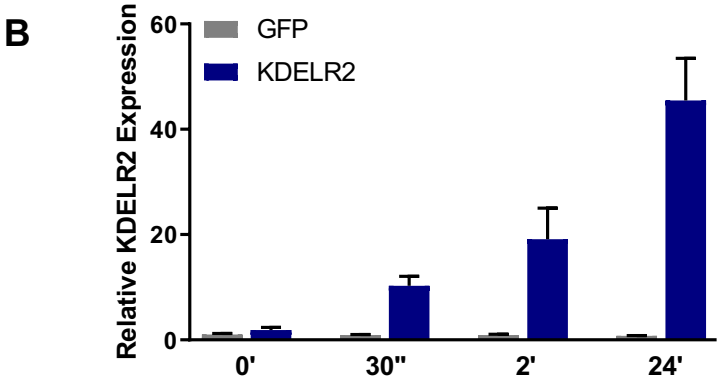


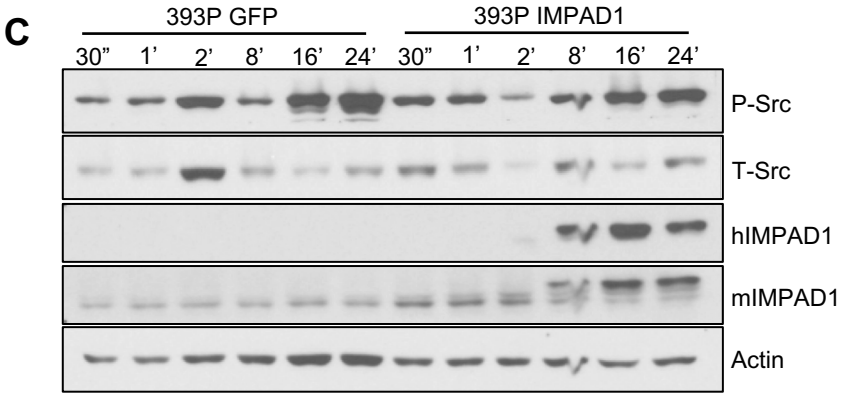

**Figure S10 KDELR2 regulates p-Src signaling**. **A** western blot showing increased Src phosphorylation within two hours of KDELR2 induction with doxycycline. **B** KDELR2 overexpression confirmed by qPCR up until 24 hours of induction. **C** Changes in Src signaling not attributed to increased IMPAD1 expression as shown by western blot.

| Gene | Sequence | Purpose | Species |
|---|---|---|---|
| IMPAD1 Forward | GTATATATAGAATTCATGGCCCCCATGGGCATCCG | Cloning | Mouse |
| IMPAD1 Reverse | CTATATATATAGAGCTCTCACTTATCGTCGTCATCCTTGTAATCATGTCCTGACTTTTCTAAATCCGG | Cloning | Mouse |
| | | | |
| IMPAD1 Forward | GTATATATAACCGGTATGGCCCCCATGGGCATCCG | Cloning | Mouse |
| IMPAD1 Reverse | CTATATATATAACGCGTTCACTTATCGTCGTCATCCTTGTAATCATGTCCTGACTTTTCTAAATCCGG | Cloning | Mouse |
| | | | |
| IMPAD1 Forward | GTATATATAGAATTCATGGCCCCCATGGGCATCCG | Cloning | Human |
| IMPAD1 Reverse | CTATATATATACTCGAGTCACTTATCGTCGTCATCCTTGTAATCATTTATGTCCTGTCTTTTCTAGATC | Cloning | Human |
| | | | |
| IMPAD1 Forward | ATGTGGATGCCTCTGACAAG | Seq | Mouse |
| IMPAD1 Reverse | CTTCTCATTGTAGGAAGAACGG | Seq | Mouse |
| | | | |
| IMPAD1 Forward | GAACACGTGGATGCAGCTGAT | Seq | Human |
| IMPAD1 Reverse | CATTGTAGGAAGAGCGGGCTT | Seq | Human |
| | | | |
| IMPAD1 Forward | CCGCAAGATGTTCTACCTGCTC | qPCR | Mouse |
| IMPAD1 Reverse | GGATGTCCTCAGGAATCTTCCG | qPCR | Mouse |
| | | | |
| IMPAD1 Forward | AATGTGAAAGCCCGCTCTTC | qPCR | Human |
| IMPAD1 Reverse | TGAAGAGCGACCTGTTTGAC | qPCR | Human |
| | | | |
| IMPAD1 SH1 | ATTCCCTAGCATATTCCAGGC | shRNA - mature antisense | Mouse |
| IMPAD1 SH2 | TTACATACTGTTAAGTACGGG | shRNA - mature antisense | Mouse |
| IMPAD1 SH3 | TTCTCATTGTAGGAAGAACGG | shRNA - mature antisense | Mouse |
| | | | |

| | | | |
|---|---|---|---|
| KDELR2 Forward | GTATTGCGAATTCATGAACATCTTCCGGCT | Cloning | Mouse |
| KDELR2 Reverse | TACAGCGTCGACTTAAACCTTATCGTCGTC | Cloning | Mouse |
| | | | |
| KDELR2 Forward | CGATACCTTCCGAGTGGAGTTC | qPCR | Mouse |
| KDELR2 Reverse | CCAGGTAGATGGAGAAGGTCCA | qPCR | Mouse |
| | | | |
| KDELR2 Forward | ACCTTCCGAGTGGAGTTTCTGG | qPCR | Human |
| KDELR2 Reverse | ATAGCCACGGACTCCAGGTAGA | qPCR | Human |
| | | | |
| KDELR2 shA | TATCGTGATTTCCATCATAGG | shRNA - mature antisense | Mouse |
| KDELR2 shB | ATCTTCAGCAGTAGGATGACG | shRNA - mature antisense | Mouse |
| KDELR2 shC | TTTCATGTAGATCAGGTACAC | shRNA - mature antisense | Mouse |
| | | | |

## Supplementary Materials

**Candidate gene selection.** We exploited microarray data collected from the KP GEM models that harbor a gain-of-function mutation in Kras, and a dominant negative mutation in p53 ($KRAS^{LA1/+}$; $p53^{R172H\Delta G/+}$). Cell lines were derived from the KP mice that could be distinguished based on their metastatic ability when they were re-implanted into the syngeneic 129/Sv mice. 393P cell lines were non-invasive, whereas 344SQ cell lines were highly invasive. Tumors from the 393P cells did not metastasize, whereas tumors from 344SQ cells metastasized to the lungs, heart, kidney, etc. The dataset that was used for human data was from the TCGA lung adenocarcinoma cohort for genes that showed >1.5-fold amplification.

***In vitro* screen and data analysis.** The 393P cell lines overexpressing individual ORFs were individually plated in quadruplicates in the tumor invasion 96-Well Plates. Randomly selected groups of 20 cell lines were seeded per plate. The plates were prepared according to manufacturer instructions (pre-warmed to room temperature (RT) for 10 minutes in 5% CO2. 75ul of warm, serum free media was added to rehydrate plates for 2 hours in). Serum free media was removed after rehydration, and cells were prepared and counted, using 15,000 cells per well, using 4 replicates per gene. 10% FBS RPMI was added to basal chamber. Invasion plates incubated for 28 hours followed by two washes with deionized water and stained with calcein AM. Cells were stained for 1 hour and fluorescence was counted on a Victor II plate reader. The fluorescence readings produced 4 raw readings per gene in each cohort. Readings were taken for 230 genes across 12 pools. The statistical analysis to identify the hits was performed by two different methods in order to minimize statistical variation and validate results. To determine the approximate expression level for each gene, while limiting the impact of experimental fluctuations, the average raw reading was calculated for each gene excluding outliers. To determine the threshold for assigning scoring genes, statistical fluctuations in the relative expression of each gene was examined relative to mCherry in each group. First, fold changes were calculated for each gene as the ratio of the gene's average reading to the average mCherry reading from the same group. To determine the amount of statistical fluctuation in fold change the standard deviation (SD) of fold change values across all genes/groups was calculated (5.89). To determine whether or not a gene's fold change was significant for the degree of statistical fluctuation in fold changes across all cohorts, each gene's fold change versus mCherry was converted into the number of standard deviations (method 1). To do this, first, for each pool, the standard deviation fold change across all pools (5.89) was converted to a raw reading basis by multiplying the standard deviation by each pool's average mCherry reading. This established 'normalized,' pool-specific standard deviation values reflective of statistical fluctuations in fold change across all pools. Second, the number of standard deviations was calculated for each gene as the ratio of the difference between the average reading for the gene and that of mCherry to the group-specific standard deviation. The number of standard deviations report the relative expression level of each gene versus an expression level equivalent to 1 standard deviation above the average expression over mCherry. To determine the final list of hits the number of standard deviations were used. It was observed that the distribution

of this metric generally followed a Gamma distribution, with most genes reporting a metric near 0 (170 out of 230) and showing positive skew. An approximate Gamma distribution was fit to the metric values for each gene with an Alpha value of 1.07 and a Beta value of 0.29. The final hit list was comprised of genes with a metric value in excess of the 90th percentile of the fit Gamma distribution (0.70).

The results from the screen were also analyzed in another way in order to minimize the statistical variation seen between cohorts (method 2). To do this, the standard deviation of the gene calculated as mentioned above, was compared to that of the mCherry in its respective cohort instead of comparing the standard deviations of the genes across that of mCherry across all groups. Those genes that had fold-change invasion greater than 3X SD of mCherry were denoted as hits. We combined the data from methods 1 and 2, and those genes that were designated as hits by both the methods were further validated.

**Migration and invasion assay.** Boyden chamber with cells plated in serum-free media added to well with complete media in the lower chamber and cells were incubated at 37 ºC for 16 hours. Inserts were stained with crystal violet and cells that migrated or invaded were quantified by using ImageJ software. Data was plotted as number of cells migrated or invaded.

**3D invasion assay.** For inducible cells were replenished everyday with RPMI media with 2% matrigel and 2uM doxycycline. Spheroids with invasive structures were imaged with an inverted microscope and quantified and plotted as %invasive structures.

**Plasmids and reagents.** EcoRI-XhoI was used for cloning IMPAD1 or KDELR2 into pTRIPZ vector. Impad1 (SH1-TRCN0000173584, SH2-TRCN0000174471, SH3-TRCN0000175469) Kdelr2 (shA- TRCN0000093585, shB-TRCN0000093586, shC-TRCN0000093588). Impad1 and Kdelr2 shRNA constructs were from GE-Dharmacon (now Horizon Discovery). Sequence for mature antisense are mentioned in Supplemental Table 1.

**qRT-PCR.** Cells were lysed in TRIzol (Ambion) and RNA was isolated from cells by using Direct-zol RNA miniprep plus kit (Zymo #R2072). cDNA was obtained by RT-PCR with 2ng/uL RNA and qScriptTM (030497, Quanta Bio). qPCR was performed with primers specific for cDNAs (Supplemental Table 1) and SYBR® Green PCR Master Mix (Life technologies).

**Western blot.** Cells and tumor tissues were lysed in RIPA buffer (Cell Signaling). Protein lysates were run by SDS-PAGE and then transferred to membrane. Protein was transferred to nitrocellulose or PVDF (only for KDELR2) membranes. 5% milk in TBST (10 mM Tris, 100 mM NaCl, and 0.1% Tween 20) was used for blocking for 1 hour at RT, except for KDELR2 where blocking was done with 5% BSA in TBST. Then probed with primary antibody overnight at 4 ºC. The primary antibodies used were: human IMPAD1 (Abcam mouse #69311, 1:1000), mouse IMPAD1 (R&D Systems sheep #AF7028, 1:1000), b-Actin (Abcam mouse), mouse KDELR2 (Abcam Rabbit #199689, 1:500), GFP (Abcam Rabbit #290, 1:1000). The secondary antibodies used were anti-mouse (Cell Signaling Technology #7076, 1:2000), anti-sheep (Santa Cruz #2770,

1:2000), anti-rabbit (Cell Signaling Technology #7074, 1:2000). All secondary antibodies were incubated for 1 hour and RT in 2.5% milk/TBS-T, except for KDELR2, which was 2.5% BSA/TBST. Blots were visualized using an ECL detection system (LF-Q0101, 27B09) from Abfrontier (Seoul, Republic of Korea).

**Wound healing assay.** Images were taken at 0 and 24 hours by using the inverted microscopy (Leica Microsystems, Germany).

**In vivo metastasis experiments.** Mice injected with doxycycline-inducible cells were fed 625mg/kg of doxycycline feed starting 48 hours after implantation of cells. Multiple comparisons ANOVA test was done for tumor growth over time curves to obtain significance for each time point. No randomization or blinding performed as only the phenotypic testing of genes was done in syngeneic mice. Mouse from 344SQ GFP cohort (Fig. 3E-J) was excluded based on PRISM outlier statistics. Mice that had no tumor growth from 393P GFP and IMPAD1 cohorts (Fig. S4Q-V) were excluded.

**Immunohistochemistry.** Formalin-fixed, paraffin-embedded tissues were cut into 4μm sections. The primary antibodies used were: mouse IMPAD1 (R&D Systems Sheep #AF7028, 1:100), FLAG (Abcam Rabbit #ab21536, 1:1000), KDELR2 (Invitrogen Rabbit #PA5-75397, 1:750). Secondary antibodies used were: anti-sheep (Abcam Rabbit #ab6746, 1:300), anti-rabbit (Dako Swine #E0353, 1:300).

**Co-immunofluorescence staining for IMPAD1 and GM130.** Primary antibody human IMPAD1 (Abcam mouse #69311, 1:100). Fluorophore-conjugated secondary antibodies: Alexa 546-conjugated anti-mouse (Thermofisher Scientific Goat #A-11030, 1:200) and GM130 (BD Pharminogen mouse #56027, 1:50).

**Co-immunofluorescence staining for KDELR2 and Calnexin, or GM130.** Primary antibody FLAG (Sigma-Aldrich Mouse #F1804, 1:1000). Fluorophore-conjugated secondary antibodies: Alexa 546-conjugated anti-mouse (Thermofisher Scientific Goat #A-11030, 1:200), Calnexin (Invitrogen mouse #MA3-027-A488, 1:100), and GM130 (BD Pharminogen mouse #56027, 1:50).

**Secretome-mediated invasion assay for Golgi secretion.** Doxycycline-induced control and experimental cells were plated in 60mm plates after 24-hour induction. Conditioned media was collected from these cells after 24 hours, where cells were treated with DMSO or 1uM BFA for the last 6 hours. 393P WT parental cells were suspended in the conditioned media and plated in invasion Boyden chambers (BD-Biosciences #354480). 50,000 cells were used per chamber. RPMI with 20% FBS was added to the lower chamber wells and the cells were incubated for 16 hours at 37 0C. Inserts were stained with crystal violet and cells that invaded were quantified by using ImageJ software. Data was plotted as number of cells invaded.

**Secretome-mediated invasion assay for MMP secretion.** Doxycycline-induced control and experimental cells were plated in 60mm plates after 24-hour of pre-induction. Conditioned media was collected after 24 hours of induction and 50,000 393P WT parental cells were plated in the

invasion Boyden chamber per well (BD-Biosciences #354480), suspended in the conditioned media. DMSO or 1uM Ilomastat was added to the invasion Boyden chambers. RPMI with 20% FBS was added to the lower chamber wells and the cells were incubated for 16 hours at 37 0C. Inserts were stained with crystal violet and cells that invaded were quantified by using ImageJ software. Data was plotted as number of cells invaded.

**Conditioned media western blot.** MMP1 antibody (Genetex Rabbit #GTX100534, 1:1000). MMP2 antibody (Cell Signaling Technology Rabbit #87809, 1:1000). MMP9 antibody (Invitrogen Rabbit #MA5-32705, 1:1000).